

International Journal of Physical Sciences

Volume 12 Number 1 16 January , 2017

ISSN 1992-1950



*Academic
Journals*

ABOUT IJPS

The **International Journal of Physical Sciences (IJPS)** is published weekly (one volume per year) by Academic Journals.

International Journal of Physical Sciences (IJPS) is an open access journal that publishes high-quality solicited and unsolicited articles, in English, in all Physics and chemistry including artificial intelligence, neural processing, nuclear and particle physics, geophysics, physics in medicine and biology, plasma physics, semiconductor science and technology, wireless and optical communications, materials science, energy and fuels, environmental science and technology, combinatorial chemistry, natural products, molecular therapeutics, geochemistry, cement and concrete research, metallurgy, crystallography and computer-aided materials design. All articles published in IJPS are peer-reviewed.

Contact Us

Editorial Office: ijps@academicjournals.org

Help Desk: helpdesk@academicjournals.org

Website: <http://www.academicjournals.org/journal/IJPS>

Submit manuscript online <http://ms.academicjournals.me/>

Editors

Prof. Sanjay Misra

*Department of Computer Engineering, School of Information and Communication Technology
Federal University of Technology, Minna,
Nigeria.*

Prof. Songjun Li

*School of Materials Science and Engineering,
Jiangsu University,
Zhenjiang,
China*

Dr. G. Suresh Kumar

*Senior Scientist and Head Biophysical Chemistry
Division Indian Institute of Chemical Biology
(IICB)(CSIR, Govt. of India),
Kolkata 700 032,
INDIA.*

Dr. Remi Adewumi Oluyinka

*Senior Lecturer,
School of Computer Science
Westville Campus
University of KwaZulu-Natal
Private Bag X54001
Durban 4000
South Africa.*

Prof. Hyo Choi

*Graduate School
Gangneung-Wonju National University
Gangneung,
Gangwondo 210-702, Korea*

Prof. Kui Yu Zhang

*Laboratoire de Microscopies et d'Etude de
Nanostructures (LMEN)
Département de Physique, Université de Reims,
B.P. 1039. 51687,
Reims cedex,
France.*

Prof. R. Vittal

*Research Professor,
Department of Chemistry and Molecular
Engineering
Korea University, Seoul 136-701,
Korea.*

Prof Mohamed Bououdina

*Director of the Nanotechnology Centre
University of Bahrain
PO Box 32038,
Kingdom of Bahrain*

Prof. Geoffrey Mitchell

*School of Mathematics,
Meteorology and Physics
Centre for Advanced Microscopy
University of Reading Whiteknights,
Reading RG6 6AF
United Kingdom.*

Prof. Xiao-Li Yang

*School of Civil Engineering,
Central South University,
Hunan 410075,
China*

Dr. Sushil Kumar

*Geophysics Group,
Wadia Institute of Himalayan Geology,
P.B. No. 74 Dehra Dun - 248001(UC)
India.*

Prof. Suleyman KORKUT

*Duzce University
Faculty of Forestry
Department of Forest Industrial Engineering
Beciyorukler Campus 81620
Duzce-Turkey*

Prof. Nazmul Islam

*Department of Basic Sciences &
Humanities/Chemistry,
Techno Global-Balurghat, Mangalpur, Near District
Jail P.O: Beltalpark, P.S: Balurghat, Dist.: South
Dinajpur,
Pin: 733103,India.*

Prof. Dr. Ismail Musirin

*Centre for Electrical Power Engineering Studies
(CEPES), Faculty of Electrical Engineering, Universiti
Teknologi Mara,
40450 Shah Alam,
Selangor, Malaysia*

Prof. Mohamed A. Amr

*Nuclear Physic Department, Atomic Energy Authority
Cairo 13759,
Egypt.*

Dr. Armin Shams

*Artificial Intelligence Group,
Computer Science Department,
The University of Manchester.*

Editorial Board

Prof. Salah M. El-Sayed

*Mathematics. Department of Scientific Computing,
Faculty of Computers and Informatics,
Benha University. Benha ,
Egypt.*

Dr. Rowdra Ghatak

*Associate Professor
Electronics and Communication Engineering Dept.,
National Institute of Technology Durgapur
Durgapur West Bengal*

Prof. Fong-Gong Wu

*College of Planning and Design, National Cheng Kung
University
Taiwan*

Dr. Abha Mishra.

*Senior Research Specialist & Affiliated Faculty.
Thailand*

Dr. Madad Khan

*Head
Department of Mathematics
COMSATS University of Science and Technology
Abbottabad, Pakistan*

Prof. Yuan-Shyi Peter Chiu

*Department of Industrial Engineering & Management
Chaoyang University of Technology
Taichung, Taiwan*

Dr. M. R. Pahlavani,

*Head, Department of Nuclear physics,
Mazandaran University,
Babolsar-Iran*

Dr. Subir Das,

*Department of Applied Mathematics,
Institute of Technology, Banaras Hindu University,
Varanasi*

Dr. Anna Oleksy

*Department of Chemistry
University of Gothenburg
Gothenburg,
Sweden*

Prof. Gin-Rong Liu,

*Center for Space and Remote Sensing Research
National Central University, Chung-Li,
Taiwan 32001*

Prof. Mohammed H. T. Qari

*Department of Structural geology and remote sensing
Faculty of Earth Sciences
King Abdulaziz University Jeddah,
Saudi Arabia*

Dr. Jyhwen Wang,

*Department of Engineering Technology and Industrial
Distribution
Department of Mechanical Engineering
Texas A&M University
College Station,*

Prof. N. V. Sastry

*Department of Chemistry
Sardar Patel University
Vallabh Vidyanagar
Gujarat, India*

Dr. Edilson Fereda

*Graduate Program on Knowledge Management and IT,
Catholic University of Brasilia,
Brazil*

Dr. F. H. Chang

*Department of Leisure, Recreation and Tourism
Management,
Tzu Hui Institute of Technology, Pingtung 926,
Taiwan (R.O.C.)*

Prof. Annapurna P.Patil,

*Department of Computer Science and Engineering,
M.S. Ramaiah Institute of Technology, Bangalore-54,
India.*

Dr. Ricardo Martinho

*Department of Informatics Engineering, School of
Technology and Management, Polytechnic Institute of
Leiria, Rua General Norton de Matos, Apartado 4133, 2411-
901 Leiria,
Portugal.*

Dr Driss Miloud

*University of mascara /Algeria
Laboratory of Sciences and Technology of Water
Faculty of Sciences and the Technology
Department of Science and Technology
Algeria*

Prof. Bidyut Saha,

*Chemistry Department, Burdwan University, WB,
India*

ARTICLES

| | |
|--|-----------|
| Multiples in Onshore Niger Delta from 3D prestack seismic data | 1 |
| G. B. Azuoko, C. N. Ehirim, J. O. Ebeniro and D. N. Uraechu | |
| Calibration and estimation of efficiency of Geiger Muller counter using a standard radioactive source | 8 |
| Vidhya Sivasailanathan, Prabhat Kumar and Suresh Sagadevan | |
| Energy saving by applying the fuzzy cognitive map control in controlling the temperature and humidity of room | 13 |
| Farinaz Behrooz, Abdul Rahman Ramli, Khairulmizam Samsudin and Hossein Eliasi | |

Full Length Research Paper

Multiples in Onshore Niger Delta from 3D prestack seismic data

G. B. Azuoko¹, C. N. Ehirim^{1*}, J. O. Ebeniro¹ and D. N. Uraechu²

¹Geophysics Research Group, Department of Physics, University of Port Harcourt, P. O. Box 122, Choba, Port Harcourt, Nigeria.

²The Shell Petroleum Development Company Port Harcourt, Nigeria.

Received 5 September, 2016; Accepted 24 October, 2016

The presence of multiples has been investigated in Onshore Niger Delta using 3D seismic data. The aim of the study was to investigate the characteristics of reflection events beyond 3s two way time on seismic data behind the boundary faults associated with the shadow zone. This involves detailed velocity analysis on semblance plot panel and accounting for moveouts due to reflections away and within the shadow zone. Interval velocity-depth models were generated from the velocity analysis and analyzed for shadow effect in the data. Results of the study revealed the presence of two velocity scenarios Onshore Niger delta. These are the primary and lower than normal velocities away and within the shadow zone, respectively. The interval velocity-depth models and their overlays on the seismic show a constant increase of velocity with depth for the primary model which seems normal, but this is contrary to the lower than normal velocity model where low seismic velocities predominate beyond 3s two way time (3.8 km), especially at the footwall of the boundary fault. These variations are likely due to the fact that sediments at the footwall of the boundary fault are thicker, compacted and thus yield stronger reflectors than the corresponding sediments away from the faults. The lower than normal velocity reflections in the absence of overpressure and anisotropy, which are also causes of low velocity reflections, are attributed to interbed multiple reflections in the data.

Key words: Seismic velocity, primary reflections, multiple reflections, boundary fault, multiple generators.

INTRODUCTION

The presence of interbed multiples in onshore Niger Delta has not until recently received attention, due to its impact on the quality and resolution of seismic reflection data. Multiples are seismic energies that have been reflected more than once before being recorded by receivers. They are known to have short periods, low

velocities and amplitudes than the desired primary reflection signals. Because of these characteristics, they are not readily distinguishable from primaries, since they have almost the same arrival time and exhibit a dispersed character that creates a curtain of noise often stronger than the primary events (Retailleau et al., 2012).

*Corresponding author. E-mail: ehirimcn@yahoo.com.

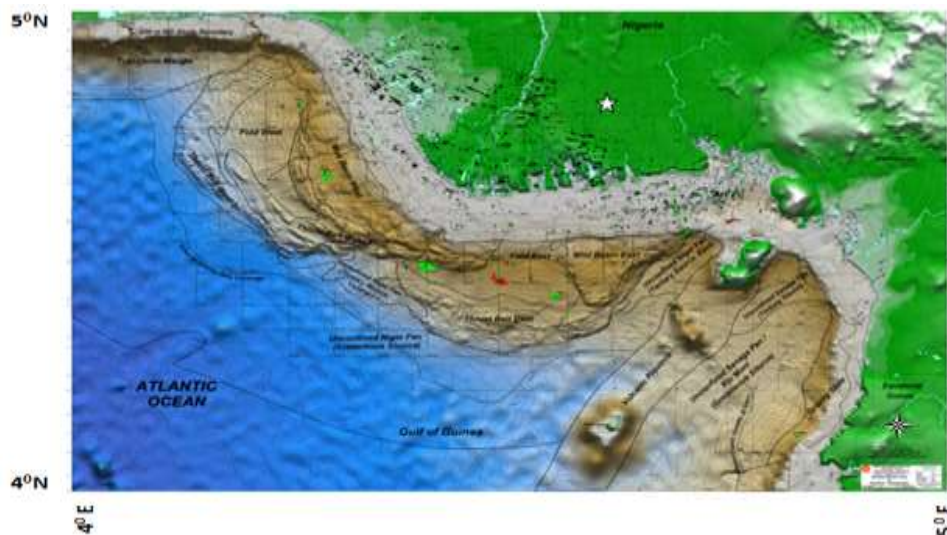


Figure 1. Location map of the study area-the white star; the study area lies within the given coordinates (Redrawn from SPDC Geosolutions Department).

The study area is located in an onshore field in southeastern Niger Delta (Figure 1). The field lies between longitude 4° and 5°E and latitudes 4° and 5°N. Seismic data from the field are often characterized by chaotic and distorted reflections beyond 3s two way time, even after detailed conditioning and processing workflows have been implemented. These distorted zones often time referred to as the fault shadow zones on seismic is situated at the footwall of main boundary faults. Due to insufficient information about their character, efforts made to remove them to enhance interpretation of data leads to loss of the desired seismic reflection signals. Away from the boundary faults, reflections are observed to be more continuous and stratigraphic definition becomes more meaningful.

Some authors have researched on the possible causes of seismic reflection distortions (Fault shadow) beyond 3s in Onshore Niger Delta. Aikulola et al. (2010) and Opara (2012) investigated overpressure as the possible cause of reflection distortions beyond 3s in Onshore Niger Delta. In a similar study, Oni et al. (2011) and Kanu et al. (2014) investigated seismic anisotropy as the possible cause of reflection distortions beyond 3s in Onshore Niger Delta. The authors in both studies noted that reflection distortions around the shadow zone exhibits lower than normal seismic velocities, which may likely be due to overpressure or anisotropy. However, accounting for these in subsequent processing work flows did not significantly improve reflections in the shadow zone.

According to Dutta (2002), secondary low velocity semblance plots represent optimum stacking velocities for multiples, but added that it has to be established not to be as a result of lithological changes or from abnormal pore pressure. Weiglein et al. (2011) also proposed that

interbed multiples can be generated by stronger subsurface reflectors regarded as multiple generators at any depth, more especially, the presence of geologic contacts of differing compactions on the footwall of main boundary faults.

Interbed multiple reflections Onshore Niger Delta has remained an exploration problem and no processing approach has so far considered in detail secondary reflections in the fault shadow zone. This attempt is therefore the first of its kind to the knowledge of the authors in Onshore Niger Delta. In the present study, we investigated the presence of interbed multiples in onshore seismic data through detailed velocity analysis of a 3D seismic data on a semblance plot panel. The study accounted for moveouts due to reflections by detailed velocity picking on the section and in the neighborhood of the shadow zone. Depth models were subsequently generated from these velocities and used to analyze the shadow zone.

GEOLOGY OF THE STUDY AREA

Generally, the geology of southwestern Cameroun and southeastern Nigeria delineates the onshore portion of the Niger Delta province (Figure 2). The Niger Delta sedimentary basin has been the scene of three depositional cycles. The first began with a marine incursion in the middle Cretaceous and was terminated by a mild folding phase in Santonian time. The second included the growth of a proto-Niger Delta during the Late Cretaceous and ended in a major Paleocene marine transgression. The third cycle, from Eocene to recent, marked the continuous growth of the main Niger Delta

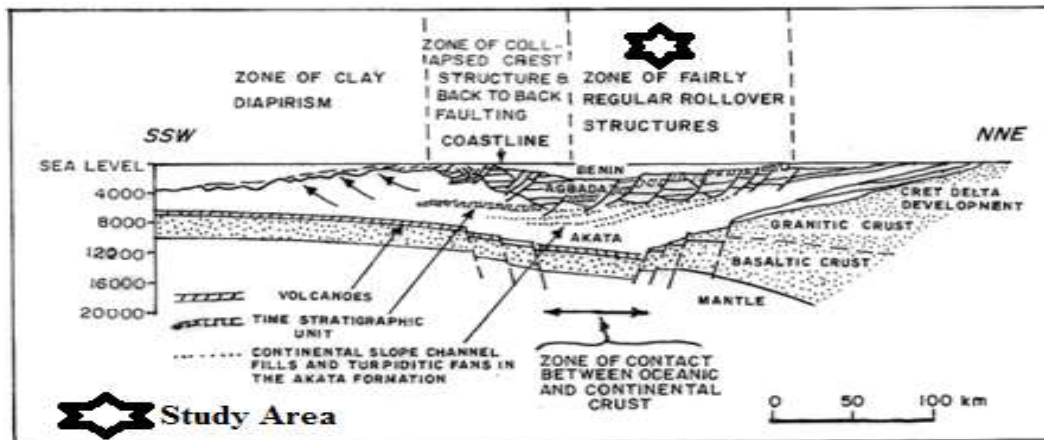


Figure 2. Tectonic and geologic section of the Niger Delta (www.intechopen.com).

(Doust and Omatsola, 1990). These cycles (depo-belts) are 30 to 60 km wide, prograde southwestward 250 km over oceanic crust into the Gulf of Guinea (Stacher, 1995), and are defined by syn-sedimentary faulting that occurred in response to variable rates of subsidence and sediment supply (Doust and Omatsola, 1990).

The interplay of subsidence and supply rates resulted in deposition of discrete depobelts. When further crustal subsidence of the basin could no longer be accommodated, the focus of sediment deposition shifted seaward, forming a new depobelt (Doust and Omatsola, 1990). Each depobelt is a separate unit that corresponds to a break in regional dip of the delta and is bounded landward by growth faults and seaward by large counter-regional faults or the growth fault of the next seaward belt" (Evamy et al., 1978; Doust and Omatsola, 1990).

Regionally, extensive anticlines and faults on the down thrown part of regional faults dip southward. These regional faults which controlled deposition (Haack et al., 2000) are of interest in this study. This is because the reflection distortions observed on seismic data exists at the footwall of these faults. The footwall of these main boundary faults has thick and compacted overburden with stronger reflectors than the up-thrown side of the fault. This configuration is known to create adequate acoustic impedance contrast, a condition necessary for the occurrence of interbed multiples in Onshore Niger Delta (Weiglein et al., 2011).

The Akata, Agbada and the Benin formations are the major stratigraphic units of the tertiary Niger Delta (Doust and Omatsola, 1990; Reijers et al., 1997). Hydrocarbon accumulation occurs in the sandstone reservoirs of the Agbada formation, within the anticlinal structures in front of growth faults (Stauble and Short, 1967; Michele et al., 1999). The typically over pressured Akata formation at the base of the delta is of marine origin and is composed of thick shale sequences (potential source rock), turbidite sand (potential reservoirs in deep water), and minor

amounts of clay and silt (Doust and Omatsola, 1990). The Benin formation is a deposit of alluvial and upper coastal plain sands that are up to 2,000 m thick and main water bearing formation in the Niger Delta (Avbovbo, 1978).

MATERIALS AND METHODS

A 3D seismic data was used in this study. The data was acquired recently using novel acquisition parameters to enhance resolution and signal-to-noise ratio (S/N). Figure 3 is atypical section showing the fault shadow zone (red circle), the main boundary fault and a line indicating the 3s two way time beyond which the distortions are observed in the study.

The semblance velocity analysis tool is sensitive to the variation of velocity with depth. In this tool, as the maximum offset increases, the semblance power decreases, since the best-fit hyperbolic moveout does not simulate the actual non-hyperbolic moveout (Alkhalifah, 1997). This tool flattens primaries within the gathers and over corrects the gathers for low velocity reflection events

Prior to the deployment of the velocity semblance tool, standard data preparation and enhancement procedures were carried out to further enhance the signal-to-noise ratio. Subsequently, velocity semblance plots were generated from common image point (CIP) gathers for detailed velocity analysis. By considering the gradual increase of effective velocity with depth, velocities were picked on the semblance plot window comprising of two panels, A and B which are respectively plots of effective velocity and offset versus time seismic data. Primary and lower than normal velocities were picked separately on panel A, while observing the moveout of the gathers on panel B away and within the shadow zone.

These velocities were picked manually by steering the pickings away from the clusters corresponding to shadow zone and observing the effect of the picking on panel B. This process was repeated for the shadow zone and observing the effect of the picking on panel B. These pickings were validated by tying them to the corresponding locations on the seismic and time slice extracted at 3 s from the data to ensure geological plausibility of the picked velocities. The picked velocities were further converted from effective to interval velocities and subsequently, interval velocity depth models were separately generated for the primary and lower than normal velocity events. These velocity models were then overlaid on the seismic section for actual mapping of anomalously low seismic velocities in the study.

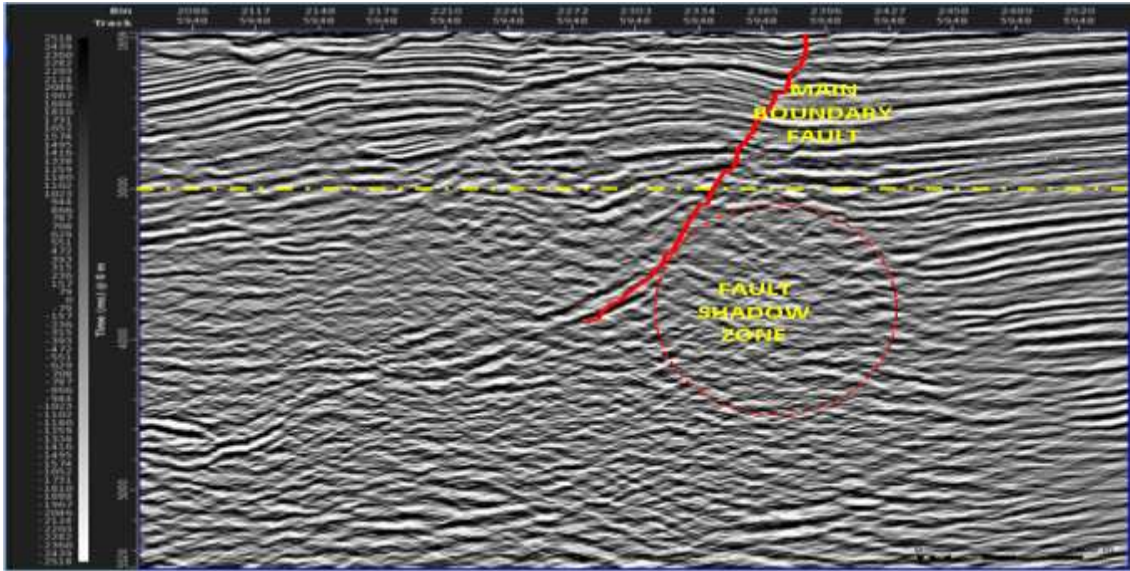


Figure 3. Typical 3D seismic section for the study showing the main boundary fault, the fault shadow zone and the 3 second two way time.

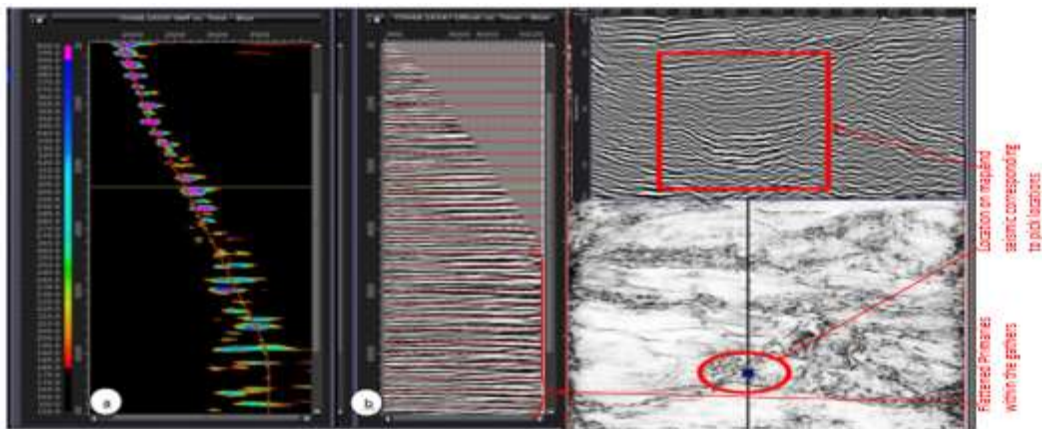


Figure 4. Picking of primary velocities away from the "shadowzone" (red rectangle).

PRESENTATION OF RESULTS

Results show that picking primary velocities (Figure 4a) flattened the offset gathers (Figure 4b) on the velocity semblance analysis window. Areas where primary reflections are predominant on the semblance plot panel correspond to areas of continuous seismic reflection events on seismic (red rectangle), which can be tied to the time slice (red circle). Moving away from the main boundary fault, reflection events become more continuous, less chaotic and distorted.

Secondary reflection events were identified as semblance clusters (or plots) corresponding to low effective velocities on the velocity semblance analysis

window (Figure 5a). Observe the upward curving "events" on the offset gathers (Figure 5b). These events travel with lower than normal velocities, which overcorrect the primary reflection events on the gathers. The locations at which this lower than normal velocities were observed and picked correlate with the shadow zone on the seismic data.

Interval velocity models built from the velocity function for primary and lower than normal velocity events are as shown in Figures 6 and 7, respectively. Figure 6 shows the normal increase of velocity with depth for the primary model. The prevalence of slower than normal velocities beyond 3.8 km (3 s) is evident in the lower than normal velocity event model (Figure 7). Note the localized nature

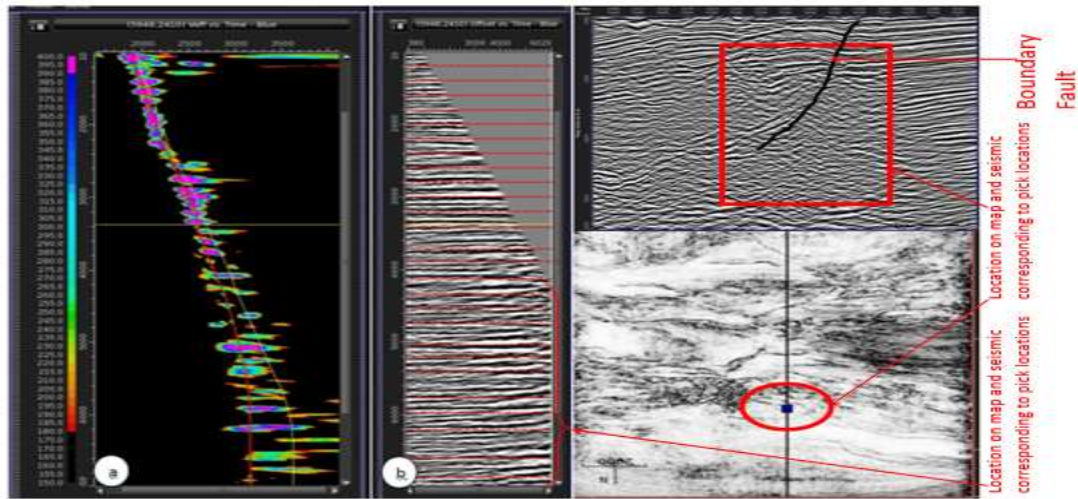


Figure 5. Picking of anomalously low velocities within the "shadow zone" (red rectangle).

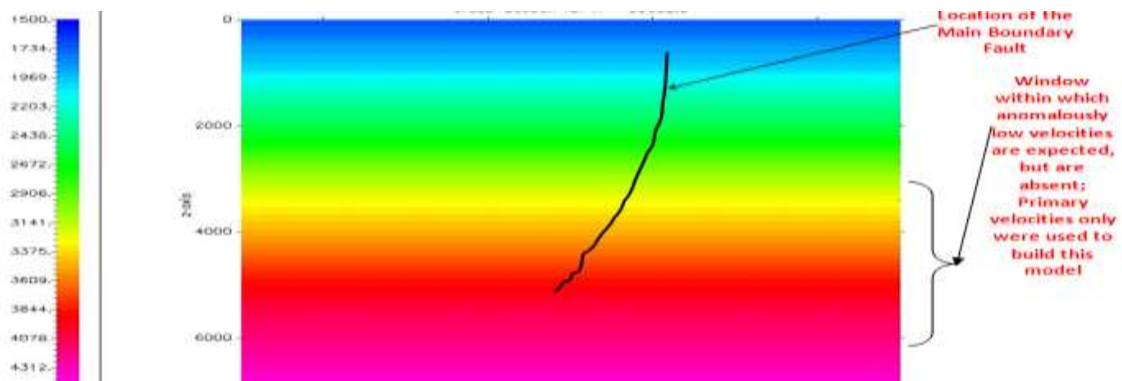


Figure 6. Velocity/Depth model showing the increase of velocity with depth for primary events.

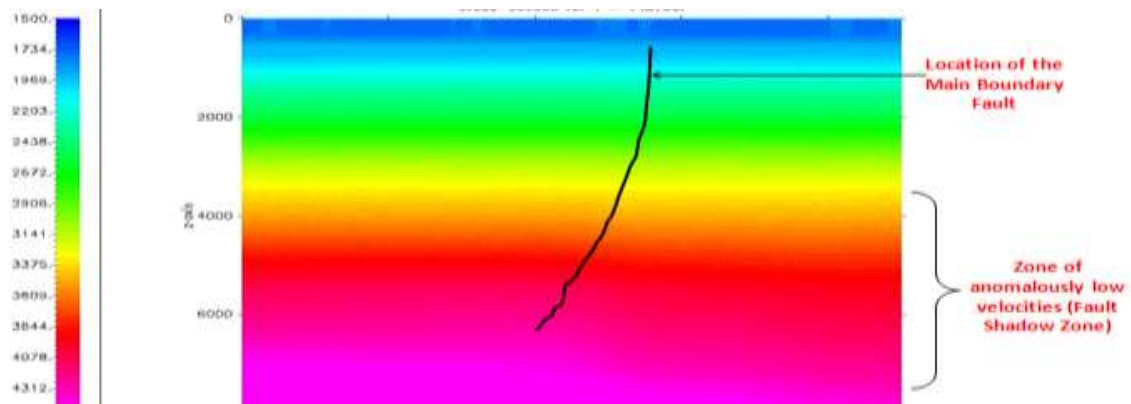


Figure 7. Velocity/Depth model showing anomalously low velocity with depth for secondary events.

of these anomalous velocities to the area corresponding to the location of the footwall of the main boundary fault

on the seismic.

Constant increase of velocity with depth is observed in

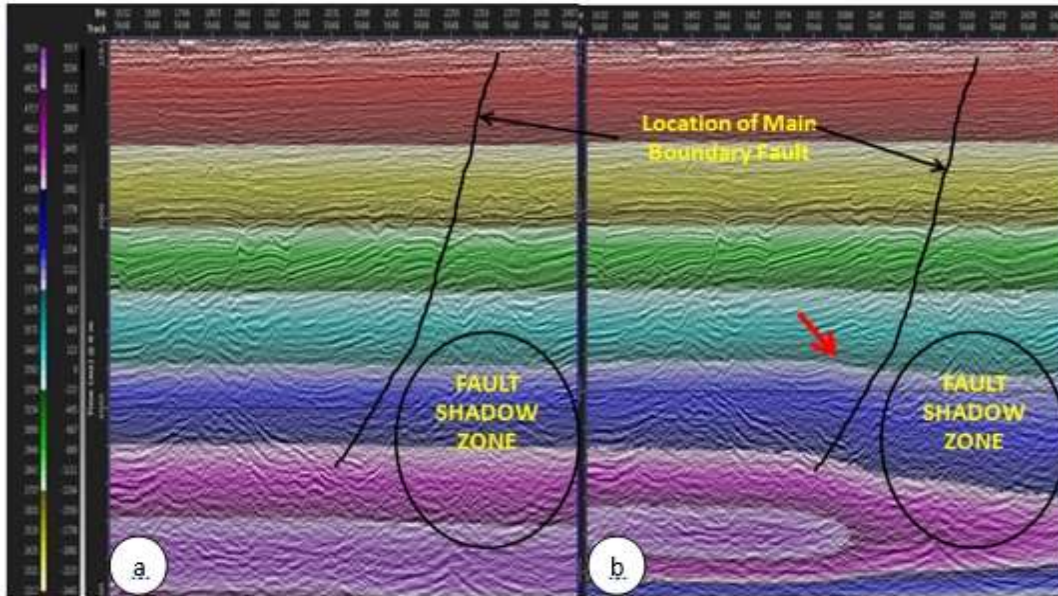


Figure 8. Overlay of interval velocity depth models for primaries (a) and lower than normal velocity events, (b) on seismic.

the overlay of the primary model on seismic (Figure 8a). In the overlay of the lower than normal velocity model on seismic (Figure 8b), we also observed constant increase of velocity with depth from 0 s to about 3 s. Beyond this two way time and in the area corresponding to the footwall of the main boundary fault, anomalously low seismic velocities were observed. This is shown by the dip in colorations towards the footwall of the main boundary fault on the figure.

This correlates with the region of the seismic section with distorted and non-continuous reflections. The red arrow in Figure 8b indicates the onset of the lower than normal velocity events.

DISCUSSION

Multiples in Onshore Niger Delta have been investigated through semblance velocity analysis of a 3D seismic data. This involves picking of reflection events in the area of interest (AOI) on the seismic data. Results revealed that picking of the right primary velocities during velocity analysis flattened the gathers and these are more predominant in locations on the seismic away from the footwall of the main boundary fault, while velocities picked around the footwall of the boundary fault; however, overcorrect reflection gathers. This suggests that these reflection events are associated with anomalously low interval velocities than the primary events.

The interval velocity-depth models and their overlays on the seismic further validate the occurrence of this

lower than normal velocity reflection events on the seismic. Constant increase of velocity with depth as observed on the primary model and overlay seems normal, but this is contrary to the velocity variation with depth delineated beyond 3 s two way time (3.8 km) on the lower than normal velocity model, especially at the footwall of the boundary fault with chaotic and distorted reflections on the seismic.

These chaotic and distorted reflections around the shadow zone are attributed to the fact that firstly, sediments at the footwall of the boundary fault are thicker, compacted and stronger reflectors than the corresponding sediments at hanging wall of the fault. These stronger reflectors referred to as multiple generators (Weiglein et al., 2011), are identified as significant sources of interbed short period multiples. Secondly, velocity estimations within the shadow zone did not properly account for this lower than normal velocities during data processing and this is likely responsible for the curtain of noise observed in the shadow zone (Retailleau et al., 2012).

Aikulola et al. (2010) related chaotic and distortive reflections observed beyond 3 s at the footwall of regional faults in the delta exhibits lower than normal seismic velocities, and associated these to the onset of overpressure regimes. Oni et al. (2011), in an onshore study in the Niger Delta, submitted that if anisotropy is taken into consideration and corrected during data preparation and enhancement, seismic imaging could be improved behind the fault. Kanu et al. (2014) reviewed velocity anisotropy considerations using different eta values. However, subsequent data processing after these

considerations did not significantly improve imaging behind the fault. Although, the works of these researchers generally impacted seismic imaging, we still had poor imaging of seismic reflections beyond 3 s. Thus, having considered and eliminated overpressure and anisotropy as the likely causes of the shadow zone, interbed multiples which are low velocities events are speculated as the possible cause of shadow effects in this study.

Furthermore, all analysis so far has blindly assumed that multiples are inexistent Onshore Niger Delta and as such, no study has fully explored the possibility of multiples being responsible for the poor imaging within the shadow zone. Based on the foregoing discussion, these lower than normal velocity events in this study could therefore be attributed to interbed multiple reflections.

Conclusions

Detailed velocity analysis of 3D seismic data on a semblance plot revealed the presence of two velocity scenarios Onshore Niger Delta. These are the primary and lower than normal velocities predominantly found away and within the shadow zone, respectively. The lower than normal velocity reflections beyond 3 s two way time in the absence of overpressure and anisotropy, which also are causes of low velocity reflections, are attributed to interbed multiple reflections in the study area. We therefore recommend carrying out depth migration with this lower than normal velocities, preferably in the prestack domain to account for reflections at the footwall of the fault in the shadow zone. This will aid attempts to attenuate the multiples and enhance stratigraphy and structure within the fault shadow zone.

However, the challenge lies in the fact that the semblance velocity analysis, as employed in this study, involved detailed velocity picking as against the automatic picking that assumes already established regional parameters. This approach gives one advantage of adequately accounting for the velocities of the chaotic reflections beyond 3s in the study area.

Conflict of Interests

The authors have not declared any conflict of interests.

REFERENCES

- Aikulola UO, Olotu SO, Yamusa I (2010). Investigating Fault Shadow s in the Niger Delta: *TLE* 16-22.
- Alkhalifa T (1997). Velocity analysis using non-hyperbolic moveout in transversely isotropic media. *Geophysics* 62(6):1839-1854.
- Avbovbo AA (1978). Tertiary Lithostratigraphy of Niger Delta. *Am. Assoc. Pet. Geol.* 62:295-300.
- Dutta NC (2002). Geopressure prediction using seismic data: Current status and the road ahead -Y2K Review Article. *Geophysics* 67(6):2012-2041.
- Doust H, Omatsola E (1990). Niger Delta: AAPG Memoir 48: Tulsa. *Am. Assoc. Pet. Geol.* pp. 239-248.
- Evamy BD, Herebourne J, Kameling P, Knap WA, Molley FA, Row lands PH (1978). Hydrocarbon Habitat of Tertiary Niger Delta. *Am. Assoc. Pet. Geol. Bull.* 62:1-39.
- Haack RC, Sundararaman P, Diedjomahor JO, Xiao H, Grant NJ, May ED, Kelsch K (2000). Niger Delta Petroleum Systems, Nigeria. *AAPG Memoir* 73: Am. Assoc. Pet. Geol. pp. 213 -231.
- Kanu M, Madiba G, Emakpor J, Olotu S, Mbah R, Obilaja S (2014). Demystifying the Fault Shadow Challenge in Onshore Nigeria. *Shell Petroleum Development Company, Port Harcourt Nigeria.*
- Michele LWT, Ronald RC, Michael EB (1999). The Niger Delta Petroleum System: Niger Delta Province, Nigeria, Cameroon, and Equatorial Guinea, Africa.
- Oni AA, Madiba G, Bertram MO (2011). Anisotropic Imaging of Okubotin 3D, Onshore Niger Delta, Article, January, 2011 www.researchgate.net
- Opara NC (2012). Investigating Abnormally Low Seismic Velocities Onshore Niger Delta within Overpressure Zones: SPDC Internship Report.
- Retailleau MG, Benjamin N, Pica A, Bendjaballah M, Plasterie P, Leroy S, Delmas L, Hugonnet P, Khalil A, Gulunay N, Smith R, Shorter J (2012). Advanced 3D Land Internal Multiple Modeling and Subtraction, A WAZ Oman Case Study. 74th EAGE Conference & Exhibition incorporating SPE EUROPEC 2012 Copenhagen, Denmark.
- Reijers TJA, Petters SW, Nwajide CS (1997). The Niger Delta Basin, in Selley, R.C., ed., *African Basins – Sedimentary Basin of the World 3: Amsterdam. Elsevier Sci.* pp. 151-172.
- Stauble AJ, Short KC (1967). Outline of Geology of Niger Delta: *Am. Assoc. Pet. Geol. Bull.* P 51.
- Stacher P (1995). Present Understanding of the Niger Delta Hydrocarbon Habitat. in Oti MN, Postma G, eds., *Geology of Deltas: Rotterdam.*
- Weiglein AB, Hsu SY, Terenghi P, Li X, Stolt RH (2011). Multiple Attenuation: Recent Advances and the Road Ahead: The Leading Edge, August, 2011.

Full Length Research Paper

Calibration and estimation of efficiency of Geiger Muller counter using a standard radioactive source

Vidhya Sivasailanathan^{1,2}, Prabhat Kumar¹ and Suresh Sagadevan^{2*}

¹Bharatiya Nabhiya Vidyut Nigam Limited, Department of Atomic Energy, Kalpakkam – 603 102, Tamil Nadu, India.

²Department of Physics, AMET University, Chennai – 603 112, India.

Received 24 September, 2016; Accepted 5 December, 2016

The beta counting system uses a Geiger-Muller (GM) tube to detect the presence of beta contamination present in filter paper samples or in planchet samples. The counting system is enabled with a provision to count the samples at various distances from the detector to the sample position. The efficiency of the counting system is provided by the manufacturer at the time of procurement which is calibrated and tested using the standardized source. The user end has to be in conformity that the counting system responds to the radioactivity properly, since efficiency acts as the standard of comparison to check the healthiness of the detector. The paper brings out the practical experience gained while validating the efficiency of the counting system at various distances using the slit height adjustment.

Key words: Efficiency, standardized source, counting system.

INTRODUCTION

The applications of nuclear techniques present a particular interest by monitoring the alpha and beta radioactive concentration from environmental factors, biological and food samples, ores samples, radioactive waste, phosphogypse deposits from industry, etc (Marian et al., 2013). Uranium concentration in soil samples have been measured by two different methods (Baykara et al., 2007), besides, Kucukomeroglu et al. (2008) investigated gross alpha/beta analyses in water by liquid scintillation counting (Wong et al., 2005) and in IAEA (2004) have

measured radioactivity in sediments. In this type of nuclear applications, the characterization of gross alpha and beta radionuclide content (Zapata-Garcia et al., 2009) can be performed for various samples: solids, liquids, aerosols filters, etc. This is the commonly used procedure in many laboratories for monitoring environmental radioactivity in various samples, first is to measure the gross alpha and beta activities and only if the results of this measurement are greater than certain prefixed limits, then other actions are performed, such as

*Corresponding author. E-mail: sureshsagadevan@gmail.com.

Author(s) agree that this article remain permanently open access under the terms of the [Creative Commons Attribution License 4.0 International License](https://creativecommons.org/licenses/by/4.0/)

the isotopic determination of uranium, thorium, radium, or lead radionuclides, generally, involving radiochemical treatments (Kovács et al., 2003). This procedure avoids the time consuming radiochemistry often necessary to evaluate individual radionuclides.

The presence of radioactivity in the environment is caused by naturally occurring radionuclides (terrestrial radiation) and cosmic radiation, but also by artificial radionuclides, which have been incorporated due to fallout from nuclear accidents (Kucukomeroglu et al., 2008). Radiation is non-sensory (Herman and Thomas, 2009) and the presence of radioactivity and radioactive material shall be identified by the use of radiation detection instruments only.

The contamination present on floor on any surface of the material shall be identified by taking a swipe and count it using a counting system. The presence of radioactive material where it is not desirable is known as contamination. Whenever maintenance job is undertaken or radiological component is taken out before taking up the job, it is required to measure the radioactivity present on the surface. The contamination along the surface also needs to be checked and in case any contamination is present, it needs to be decontaminated before executing the job.

Sample preparation

To find out the beta activity present in liquid samples like borewell water samples, etc., the sample need to be plancheted first. A fumehood set up is used for this purpose. The liquid sample of 10 ml is pipetted out and poured in the planchet. The sample will be dried with the help of an IR lamp inside the fumehood. After it got dried, the planchet shall be placed in the counter for counting of the activity. The study focused on the effects of variation of efficiency with respect to change in distance. The other parameters like operating voltage, strength of source and comparison with the active samples were not covered.

The purpose of this study was to present the working of the beta counting system, including the efficiency calibration of the system using standard radiation sources.

MATERIALS AND METHODS

The counting system is a device used to identify the contamination present on floor or on surface of any material. The presence of alpha and beta can be checked by taking a swipe at the area or the surface. The swipe paper shall be placed in the counting system and based on the counts observed, the presence of contamination shall be known. The beta counting system uses a GM tube for detection of presence of any beta contamination present.

Setting up of a GM counter

GM probe type GP-30 is with mica window. GM tube is used to measure beta contamination counting. A stand to mount GM tube with slits to adjust the height of sliding planchet tray provided to fix. To mount GM tube, a stand with the number of slits to adjust the height of sliding planchet tray is provided. The radiation detected by GM counter is beta. Figure 1 shows the typical working arrangement of a fully assembled beta counting system. Figures 2 and 3 are the sketch showing the lead shielding assembly and the slit arrangement with a planchet tray in the counting system.

Description of the Instrument

The instrument consists of a GM probe GP 30 with LND 7224 GM tube. The input selectivity is -50 mV pulses (Pla Electro Reports, 2013). The built in load resistor is 3.3 MΩ for GM probe. The paralysis time selection is 250 μs. The pulse height discriminator is selectable by internal preset value of 200 mV to 2.5 V. HV is a set at 500 V. The power supply applied is 230 V AC ± 10%, 50 Hz. High voltage connector is provided to connect GM probe. Signal received through this detector probes are fed to amplifier circuit and then to pulse discriminator circuit monoshot shapes. These pulses as per paralysis time selected by user signal o/p of monoshot are fed to micro controller. Microcontroller counts these pulses and displays as counts CPM or CPS.

Operating principle of the instrument

The Geiger Muller counter works on the principle of a gas filled detector (Glenn, 2000). It consists of a cylindrical tube filled with a gas and connected to an applied voltage. The interaction of the radiation with the gas present in the detector is instantaneous, typically a few nano seconds is enough in gases and pico seconds in solids, respectively to create quantifiable charge. The simplified detector model thus assumes that a charge Q appears within the detector at a time $t=0$ resulting from the interaction of a single particle or quantum of radiation. This charge manifests in electric signal that can be measured. Typically, collection of the charge is accomplished through the imposition of an electric field within the detector, which causes the positive and negative charges created by the radiation to flow in opposite directions.

Experiment

The counting system needs to be checked for the effectiveness of its calibration and its efficiency needs to be standardized using a standard radioactive source of known activity. The source was placed in the slit and the counts by the detector were observed. The counts per seconds were calculated. With the known activity (dps) and the counts observed per second (cps) were used for the calculation of efficiency. The background counts of the system would be observed and the average of the counts was taken as the background counts. The gross cps observed with the source is deducted from the average value of the background counts to arrive at the net counts per second (net cps). The efficiency thus calculated shall be used for the estimation of activity in the unknown samples of swipe or the plancheted ones.

$$\text{Efficiency } (\eta) = (\text{cps/dps}) \times 100$$



Figure 1. Working arrangement of a typical Beta counting system.

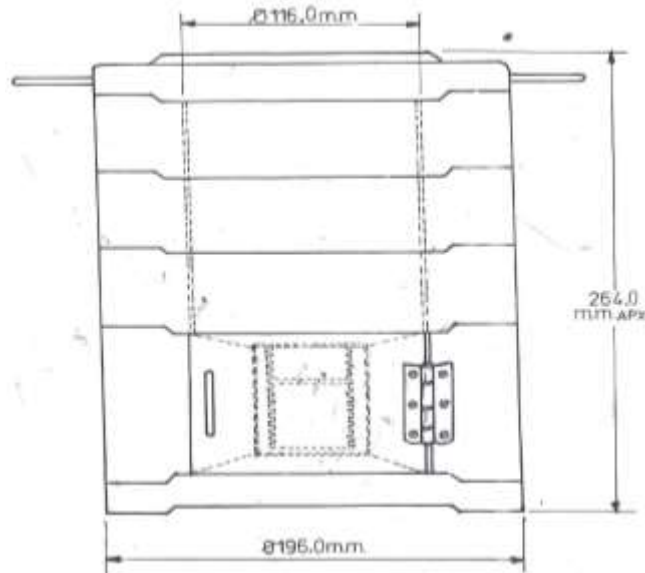


Figure 2. Lead shielding assembly for counting system.

The radioactive source of ^{90}Sr - ^{90}Y was used to carry out the experiment. The strength of the source was 3 KBq as on February 2013 (Half-life of the radioactive strontium-90 is 30 years). The operating voltage of the system was kept at 500 V throughout the experiment. The background counts were observed for 60 s and repeated for 10 times. The source was kept in second slit and the counts were observed for 60 s. The counting was repeated for 10 times. Then the source was placed in the 3rd slit and the counts were observed for 60 s and repeated for 10 times. The experiment was repeated for 10 slits similarly. The net counts were calculated by subtracting the background cps from the gross cps for each slit readings. The efficiency was calculated using net cps and the activity of the source used.

RESULTS AND DISCUSSION

The observations were tabulated and the efficiency in each slit was calculated and updated. From the Table 1, it is seen that the counts are comparatively closer to each other when the source is kept at second and third slit positions. Starting from the 4th slit, the values start decreasing. This is due to the fact that the amount of radioactivity that reaches the detector varies as the distance varies. When the activity from the source is of minimum strength, it loses its ability to ionize the

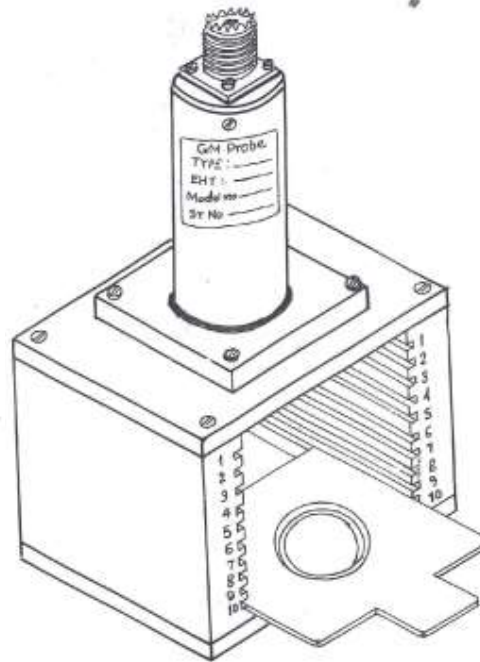


Figure 3. GM tube with height adjustable slit.

Table 1. Observations of counts with beta counting system.

| S/N | The counts observed by adjusting the height of the slits from the detector | | | | | | | | | |
|-------------|--|--------|---------|---------|--------|---------|--------|---------|--------|---------|
| | Bkgd CPM | Slit-2 | Slit-3 | Slit-4 | Slit-5 | Slit-6 | Slit-7 | Slit-8 | Slit-9 | Slit-10 |
| 1 | 9 | 20510 | 20060 | 19800 | 14500 | 13800 | 12100 | 8000 | 7200 | 5100 |
| 2 | 7 | 20515 | 20059 | 19810 | 14300 | 13790 | 12100 | 8100 | 7190 | 5150 |
| 3 | 9 | 20500 | 20060 | 19800 | 14450 | 13795 | 12110 | 8090 | 7185 | 4960 |
| 4 | 8 | 20510 | 20350 | 19810 | 14480 | 13810 | 11900 | 8100 | 7195 | 4980 |
| 5 | 11 | 20515 | 20320 | 19700 | 14500 | 13800 | 11990 | 8120 | 7200 | 5000 |
| 6 | 12 | 20510 | 20300 | 19810 | 14510 | 13810 | 12010 | 8100 | 7210 | 5050 |
| 7 | 10 | 20520 | 20010 | 19800 | 14520 | 13800 | 12090 | 8050 | 7190 | 5100 |
| 8 | 9 | 20500 | 20040 | 19805 | 14490 | 13820 | 12080 | 8100 | 7210 | 5100 |
| 9 | 9 | 20515 | 20350 | 19810 | 14580 | 13800 | 12090 | 8200 | 7196 | 5100 |
| 10 | 10 | 20515 | 20350 | 19810 | 14510 | 13810 | 12100 | 8100 | 7200 | 5100 |
| Average CPM | 9.4 | 20511 | 20189.9 | 19795.5 | 14484 | 13803.5 | 12057 | 8096 | 7197.6 | 5064 |
| Average CPS | 0.15666 | 341.85 | 336.49 | 329.925 | 241.4 | 230.058 | 200.95 | 134.933 | 119.96 | 84.4 |
| Net CPS | | 341.69 | 336.34 | 329.768 | 241.24 | 229.90 | 200.79 | 134.776 | 119.80 | 84.2433 |
| Efficiency | | 11.38 | 11.21 | 10.99 | 8.041 | 7.663 | 6.6931 | 4.4925 | 3.9934 | 2.8081 |

detector. As the number of ionizations becomes minimum, the counts observed will also be minimum. So the distant slit positions from the detector show lesser counts. The operating voltage supplied to enhance the

initial ionization becomes insufficient to raise up the ionization effect when the distance of the source increases away from the detector. The time set for the counting is also fixed as 60 s throughout the experiment.

The increased time will contribute for more ionization inside the detector. The parameters that contribute for the effective ionization inside the gas filled detectors include, applied voltage, counting time, distance of the source from the detector, energy and strength of the radionuclide, etc. The experiment is carried out only to study the effect of distance over estimation of efficiency keeping the counting time and operating voltage as a constant. This is useful for calculation of activity of any swipe samples collected from the contaminated surfaces of objects or the floor. The same can also be useful for finding the activity of beta in a liquid samples after plancheting them using infrared (IR) lamp in a fumehood set up.

Conclusion

The present study shows that the efficiency of the counting system will be higher when the height of the slit is chosen close to the detector. The efficiency of the detector depends upon the type and strength of the ionizing radiation that either the sample or the radioactive source material possesses. The increased distance chosen from the source to reach the detector or in other words, the measurement side contributes to the comparatively lesser counts. This also exhibits the "distance" concept of reducing the exposure to the occupational worker. The longer the distance, lesser the exposure will be. The sealed source used for calibration is of known strength and is kept as standard for such calculations are brought in such a way that it is plancheted on one side of the pellet. Whenever the reverse side of the pellet is placed facing the detector, the counts will be still lower. The efficiency of the detector shall be made reasonable by making the counting time longer. Thus, the estimation or determination of efficiency depends upon other parameters also like applied voltage, counting time, distance of the source from the detector, energy and strength of the radionuclide. The counting system with its efficiency calculated for the particular slit only needs to be used for the estimation of activity of the unknown samples. Otherwise, the estimated efficiency corresponding to the slit in which the sample was kept has to be taken for the estimation of activity of the sample.

Conflict of Interests

The authors have not declared any conflict of interests.

ACKNOWLEDGEMENT

The authors sincerely acknowledge the guidance and support rendered by the supervisor to bring out this paper and the management to pursue this study.

REFERENCES

- Baykara O, Kulahci F, Dogru M (2007) Measurement of uranium concentration in soil samples by two different methods. *J. Radioanal. Nucl. Chem.* 272(1):195-197.
- Glenn FK (2000). *Detection and Measurement*. Third Edition, John-Wiley & Sons Inc.
- Herrman C, Thomas EJ (2009). *Introduction to Health Physics*. Fourth Edition, McGraw-Hill Companies.
- IAEA (2004). *Radiation, People and the Environment*, printed by the IAEA in Austria, February 2004.
- Kucukomeroglu B, Kurnaz A, Keser R, Korkmaz F, Okumusoglu NT, Karahan G, Sen C, Cevik U (2008). Radioactivity in sediments and gross alpha-beta activities in surface water of Firtina River, Turkey. *Environ Geol* 55:1483-1491.
- Kovács T, Bodrogi E, Somlai J, Jobbágy V, Patak G, Nemeth Cs (2003). ²²⁶Ra and ²²²Rn concentrations of spring waters in Balaton upland of Hungary and the assessment of resulting doses. *J. Radioanal. Nucl. Chem.* 258:191-194.
- Marian RC, Alexandru ED, Ileana R (2013). The calculation of the detection efficiency in the calibration of gross alpha-beta systems. *J. Radioanal. Nucl. Chem.* 295:283-288.
- Pla Electro Reports (2013). *Reports from Pla Electro Appliances Pvt. Ltd., Mumbai.*
- Wong CT, Soliman VM, Perera SK (2005). Gross alpha/beta analyses in water by liquid scintillation counting. *J. Radioanal. Nucl. Chem.* 264(2):357-363.
- Zapata-Garcia D, Llauro M, Rauret G (2009). Establishment of a method for the rapid measurement of gross alpha and gross beta activities in sea water. *Appl. Radiat. Isot.* 67(5):978-981.

Full Length Research Paper

Energy saving by applying the fuzzy cognitive map control in controlling the temperature and humidity of room

Farinaz Behrooz^{1*}, Abdul Rahman Ramli², Khairulmizam Samsudin² and Hossein Eliasi³

¹Institute of Advanced Technology, Universiti Putra Malaysia, Serdang, Selangor - 43400, Malaysia.

²Department of Computer and Communications, Universiti Putra Malaysia, Serdang, Selangor - 43400, Malaysia.

³Department of Electricals Engineering, University of Amir Kabir, Iran.

Received 2 June, 2011; Accepted 15 July 2011

This paper investigated the implementing of soft computing methodology of fuzzy cognitive map on controlling parameters of heating, ventilating and air-conditioning systems. In the past few years, many researches have been done on application of different controllers on heating, ventilating and air-conditioning system as a more energy consuming part of the building automation system. Unlike the conventional control methods which are used more in this area like PID controller, the fuzzy cognitive maps method was chosen to control of the temperature and humidity of the room in winter operation season and summer operation season. By applying the fuzzy cognitive map controller, more energy efficiency and also more energy saving has obtained. The advantages of using fuzzy cognitive maps indicated as a controller on the typical heating, ventilating and air-conditioning system in this paper. The algorithm of FCM control reached to the goals of comfort, robustness and energy saving.

Key words: Fuzzy cognitive map, heating ventilating and air-conditioning system, energy saving, energy efficiency, robustness.

INTRODUCTION

The heating, ventilating and air-conditioning (HVAC) system is the more energy consuming part of the building automation systems (BAS) in the intelligent buildings. Due to the limited sources of energy in the world and also fuel crisis, designing the better controllers to saving

energy and energy efficiency is more important challenging for control engineers (Tachwali et al., 2007). Due to the great impact of HVACs systems on power and energy consumption, knowing the structure and operation of HVAC systems are possessing importance (Tashtoush

*Corresponding author. E-mail: fery_behrooz@yahoo.com. Tel: 006-017-6350970, 00989125272708.

Abbreviations: HVAC, Heating, ventilating and air-conditioning; BAS, building automation system; FCM, fuzzy cognitive map, FL, fuzzy logic, ANN, artificial neural network.

Author(s) agree that this article remain permanently open access under the terms of the [Creative Commons Attribution License 4.0 International License](http://creativecommons.org/licenses/by/4.0/)

et al., 2005). According to Tashtoush et al. (2005) energy efficiency and indoor climate conditions are most important goals of designing HVAC systems. As a result of complicated quality of an HVAC system, obtaining to the mathematical model of HVAC is very difficult (Tashtoush et al., 2005) and also designing the proper controller become a big challenge (Lei et al., 2006; Wang et al., 2006). Designing the suitable controller could be saved a considerable amount of energy (Huang et al., 2006).

Research contributions and motivations

Fuzzy cognitive maps (FCMs) are utilized to model the complex dynamical systems and control plants. Most of the previous works on FCMs discuss about implementation of this method on modeling the complex systems. According to Stylios and Groumpos (2004), applying FCMs as a control system make efforts toward more intelligence on control systems. In spite of the accuracy of the conventional control methods (Stein et al., 2000), intelligent control methods could modify some negative points of the conventional methods.

Applying the PID controller on HVAC systems based on Tashtoush et al. (2005) work, shows the consuming more energy due to the overshoot and undershoot which are observed, but by applying intelligent control methods overshoot and undershoot cancelling are reached. Fuzzy logic (FL) and artificial neural network (ANN) beyond the others are more usable but in FL method to obtain more accuracy, a large number of rules block required which is more time consuming and also in ANN method the volume of the mathematical calculation needs more time. Obtaining to the more accuracy and also decrease the calculation time the FCM method is chosen. The FCMs is combination of the FL method and ANN method and contain the robust characteristics of both methods (Aguilar, 2005; Stylios and Groumpos, 2000). Finally, applying the combination of control techniques of fuzzy logic and neural networks are recommended to control of buildings. The hybrid method of fuzzy logic and neural networks contain the robust characteristics of both methods. In addition, the shortcomings of both methods are omitted in this method. The robustness of FCMs is another important reason of choosing this method. Regarding to definition, characteristics and simplicity of mathematical model of FCMs, implementing the FCMs as a direct control is recommended in control the parameters in building automation systems to achieve more intelligence in building and as well more energy saving. As a result of structure of FCMs, the run time of control process is declined. Due to the ability of FCMs in having learning strategy, the consumption of energy could be decreased. Due to the fact that, the energy sources are limited and energy crisis, saving more energy is important goal of using building automation

systems. Therefore, The FCMs as a direct control system are proposed to reach the objectives of decreasing run time of control process and saving energy. Decreasing the consuming energy by HVAC system due to the eliminating of overshoots and undershoots on the supply temperature and supply humidity. On the other words, saving energy is the highlight contribution of this research.

Research objectives

Applying the FCM controller as a direct control on HVAC systems to obtain a nonlinear, robust controller and also achieving to a closed-loop, real-time and on-line learning ability controller with simple control algorithm and also fast convergence by using supervised learning are the objective of this paper. On the other words, the main objectives of this research are designing a nonlinear robust controller using Fuzzy Cognitive Map (FCM) to control the temperature and humidity of the room, to optimize and improve thermal comfort issue and Energy efficiency by obtaining the balance between thermal comfort and energy usage and designing a Closed-loop real-time on-line learning ability controller with simple control algorithm.

Description of HVAC system

As a result of increasing the population and global warming and many other serious reasons, demanding for energy saving is feasible (Tachwali et al., 2007). Due to the much consumption of energy by HVAC systems, is almost around 50% of total of generated electrical energy in the world, designing the appropriate controller for declining the consumption of energy is considerable (Tachwali et al., 2007).

A heating, ventilating and air conditioning system or on the other words HVAC system consist of number of subsystems as indoor air loop, chilled water loop, refrigerant loop, condenser water loop and outdoor air loop (Lei et al., 2006; Wang et al., 2006). HVAC systems consist of a number of nonlinear and time-varying subsystems (Wang et al., 2006). So the HVAC systems are known as typical non-linear time-variable multivariable systems with disturbances and uncertainties (Lei et al., 2006). The typical HVAC systems include of a room, humidifier, heater, cooler, fan and duct (Tashtoush et al., 2005). According to Tashtoush et al. (2005), winter operation seasons' components are the zone, duct, mixing box, heating coil and humidifier but heating coil and humidifier are replaced by cooling coil and dehumidification coil in summer operation season. Assuming the homogeneous temperature distributing in the zone, the equal effect of walls and roofs in the zone in every respect and no effect of ground, the constant air's

density, disregarding the pressure losses of interzone and the external heat sources like the number of persons and appliances as an uncontrolled inputs are considered.

Referring to Tachwali et al. (2007) and Tashtoush et al. (2005), the mathematical model of typical HVAC systems based on many studies on dynamical model of HVAC consists of the zone model, mixing box model, duct model, fan model, heating coil model, humidifier model, cooling coil model and dehumidification coil model as follows:

The rate of thermal energy change in the zone is described by Equation (1) and through the walls and roof by Equations (2 to 4) and the humidity ratio of the zone by Equation (5).

$$dT_z/dt = (\beta/c_z)(T_{sup} - T) + (2\gamma/c_z)(T_{w1} - T) + (\lambda/c_z)(T_R - T) + (2\delta/c_z)(T_{w2} - T) + (1/c_z)q(t) \quad (1)$$

$$dT_{w1}/dt = (\gamma/c_{w1})(T_z - T_{w1}) + (\gamma/c_{w1})(T_o - T_{w1}) \quad (2)$$

$$dT_{w2}/dt = (\delta/c_{w2})(T_z - T_{w2}) + (\delta/c_{w2})(T_o - T_{w2}) \quad (3)$$

$$dT_R/dt = (\lambda/c_R)(T_z - T_R) + (\lambda/c_R)(T_o - T_R) \quad (4)$$

$$dW_z/dt = (f_{sa}/V_z)(W_s - W_z) + (1/\rho_w V_z)P(t) \quad (5)$$

Where:

$$\beta = f_{sa}\rho_a C_{Pa}, \quad \gamma = U_{w1}A_{w1}, \quad \lambda = U_R A_R, \quad \delta = U_{w2}A_{w2}$$

The Equations (6) and (7) illustrate the energy and mass balance of mixing box, which outside temperature is (T_o), return temperature from the zone is (T_r), outside humidity ratio is (W_o), return humidity ratio from the zone is (W_r), mass flow rate of the outdoor air (m_o) and mass flow rate of the recalculated air (m_r).

$$T_m = (m_r T_r + m_o T_o) / (m_r + m_o) \quad (6)$$

$$W_m = (m_r W_r + m_o W_o) / (m_r + m_o) \quad (7)$$

According to the Tashtoush et al. (2005) and Clark et al. (1985) expanded the transient model for duct unit. The Equation 8 shows the rate change of air temperature of duct model. T_i is inlet air temperature and T_{out} is the exit air temperature. The h_i is heat transfer coefficient inside the duct and h_o is the heat transfer coefficient in the ambient. M_d is mass of the duct model; C_d is specific heat of the duct material; Mass flow rate of the air stream is m_a ; specific heat of air is C_{pa} .

$$dT_{out}/dt = ((h_i + h_o) m_a C_{pa}) / (h_i M_d C_d) (T_{in} - T_{out}) \quad (8)$$

Referring to the Tashtoush et al. (2005) passing the air from the fan, increasing the temperature around 1-2°C. Heating coil exchange the heat from water to air to provide prepared ventilating air in building. T_{wi} is the

temperature of supplied heating water to the heating coil. T_{wo} is the exit water temperature of heating coil. The assumptions in the heating coil part are the constant mass flow rate of the water inside coil, neglecting the thermal resistance due to the considering of high conductivity of the coil material and T_{wo} is considered to be constant and is equal to 10°C. Equation (9) shows the energy balance between hot water and cold air which rate of exchanging energy in the air passes from the coil is equal to energy which is added by the flow rate of water in the heating coil and the transferred energy by return air to the surrounding. Equation (10) indicates the mass balance.

$$C_{ah} (dT_h/dt) = f_{sw}\rho_w C_{Pw} (T_{wi} - T_{wo}) + (UA)_a (T_o - T_{co}) + f_{sa}\rho_a C_{Pa} (T_m - T_{co}) \quad (9)$$

$$V_{ah} (\sigma W_{co}/\sigma t) = f_{sa} (W_m - W_{co}) \quad (10)$$

The mass transfer of water vapor to the atmospheric air to increase the water vapor in the mixture is humidification. Due to the undesirable impacts of very low moisture content on the human body, measuring and controlling of the moisture in the air are considerable phase of air conditioning. According to Tashtoush et al. (2005), developing the energy and mass balance equations of the humidifier model by Kasahara et al. (2000) are as follows:

$$C_h (dT_h/dt) = f_{sa} C_{Pa} (T_{si} - T_h) + \alpha_h (T_o - T_h) \quad (11)$$

$$V_h (dW_h/dt) = f_{sa} (W_{si} - W_h) + (h(t)/\rho_a) \quad (12)$$

The rate of humid air, producing by humidifier and also function of humidity ratio in Equation (12), indicates by $h(t)$. Set point values of the system for winter operation season are considered as outside temperature of 5°C, outside humidity of 0.00377 kg/kg (dry air), supply temperature of 25°C, constant value of the volume flow rate of the supply air and is equal to $f_{sa} = 0.192 \text{ m}^3/\text{s}$, two lamps with load 0.5 kW and also two persons with 0.15 kW load are considered as uncontrolled inputs in the zone and the initial values of the zone temperature and zone humidity ratio when $t=0$ are equal to $T_z(0) = T_o$ and $W_z(0) = W_o$. The desired values are 22°C for zone temperature and 0.008 kg/kg for the zone humidity ratio.

The important component of air conditioning unit and also the important interface between the primary plant and the secondary air distribution system is cooling coil. Passing air through the coil in contact with the cold fin surfaces causes heat transfer from air to the water by flowing inside the tubes. Due to the significance of the cooling coil, study of the cooling coil transient behavior and its response characteristics were developed by several models. In Tashtoush et al. (2005) work, developing transient model of a chilled-water coil by Elmahdy and Mitalas (1977) is adopted. In Equations (14)

Table 1. Parameters of PID controllers in summer operation season.

| Cooling mode | Cooling coil | Dehumidifier |
|----------------|--------------|--------------|
| Gain | 2 | 5 |
| Integrator | 0.0015 | 0.0035 |
| Differentiator | 0.1 | 0.1 |

Table 2. Parameters of PID controllers in winter operation season.

| Heating mode | Heating coil | Humidifier |
|----------------|--------------|------------|
| Gain | 3 | 0.65 |
| Integrator | 0.011 | 0.008 |
| Differentiator | 25 | 10 |

and (15), T_a is air temperature and W_a is humidity ratio which are used as a function of water temperatures T_{w1} and T_{w2} respectively.

$$T_a (T_{w1}) = -0.0587(T_{w1})^2 + 1.773 (T_{w1}) + 1.1816 \quad (13)$$

$$W_a (T_{w2}) = 3.2434 \times 10^{-5} (T_{w2})^2 - 1.7972 \times 10^{-5} (T_{w2}) + 6.223 \times 10^{-3} \quad (14)$$

Validity range for Equations (13) and (14) is $T_w = 5-50^\circ\text{C}$. Set point values of the system for summer operation season are considered as outside temperature of 32°C , outside humidity of 0.01251 kg/kg (dry air), supply temperature of 13°C , constant value of the volume flow rate of the supply air and is equal to $f_{sa} = 0.192 \text{ m}^3/\text{s}$, two lamps with load 0.5 kW and also two persons with 0.15 kW load are considered as uncontrolled inputs in the zone and the initial values of the zone temperature and zone humidity ratio when $t=0$ are equal to $T_z(0) = T_o$ and $W_z(0) = W_o$. The desired values are 22°C for zone temperature and 0.008 kg/kg for the zone humidity ratio.

LITERATURE REVIEW

Here, the controller designed by Tashtoush et al. (2005) is reviewed and the PID controller was used. The values of the parameters of The PID controllers, obtained from Ziegler-Nichols method. The PID controller transfer function which was used consists of three different elements which can be described as $G_c(s) = K_p + K_i/s + K_Ds$.

Based on previous discussions about HVAC systems, the operation of the system are categorized on two different operation seasons as summer and winter. It is clear that each operation season requires two separate controllers to control temperature and humidity respectively. The Table 1 shows the parameters of the PID controller for cooling mode of summer operation

season. The other two controllers related to the heating mode of winter operation season which are related to control of temperature and humidity respectively. The Table 2 indicates the parameters of these two mentioned controllers. At the result section, the responses of the HVAC system under control of mentioned PID controller have been got and finally the results of PID controller and FCM one are compared. Figures 1 and 2 shows the results of applying PID controller based on Tashtoush et al. (2005) work.

Overview of FCM

At first time, the cognitive maps are introduced by Robert Axelord in 1976 in social and political sciences. The application of cognitive maps at first was a way to represent social scientific knowledge and model decision making in social and political systems. The applications of cognitive maps are not also in political and social sciences but also in many areas like analysis of electrical circuits, medicine, supervisory systems, organization and strategy planning, analysis of business performance indicators, software project management, information retrievals, modeling of plant control, system dynamics and complex systems and modeling virtual world, etc (Aguilar, 2005; Bertolini, 2007; Ghazanfari et al., 2007). Finally in 1986 the idea of cognitive maps were extended by Bart Kosko to fuzzy cognitive maps by replacing the numeric value of concepts with fuzzy values or on the other hands with lying the value of concepts in interval $[0, 1]$ or $[-1, 1]$ (Bertolini, 2007). Also the relationships between concepts take a value in interval $[0, 1]$ or $[-1, 1]$ (Bertolini, 2007). FCMs indicates the behavior of the system in terms of concepts which each concept stand for a situation or feature of the system (Aguilar, 2003, 2005). The whole system is shown by FCMs as a directed graph with concepts and their causal relationships in a given scenario (Khor and Khan, 2003).

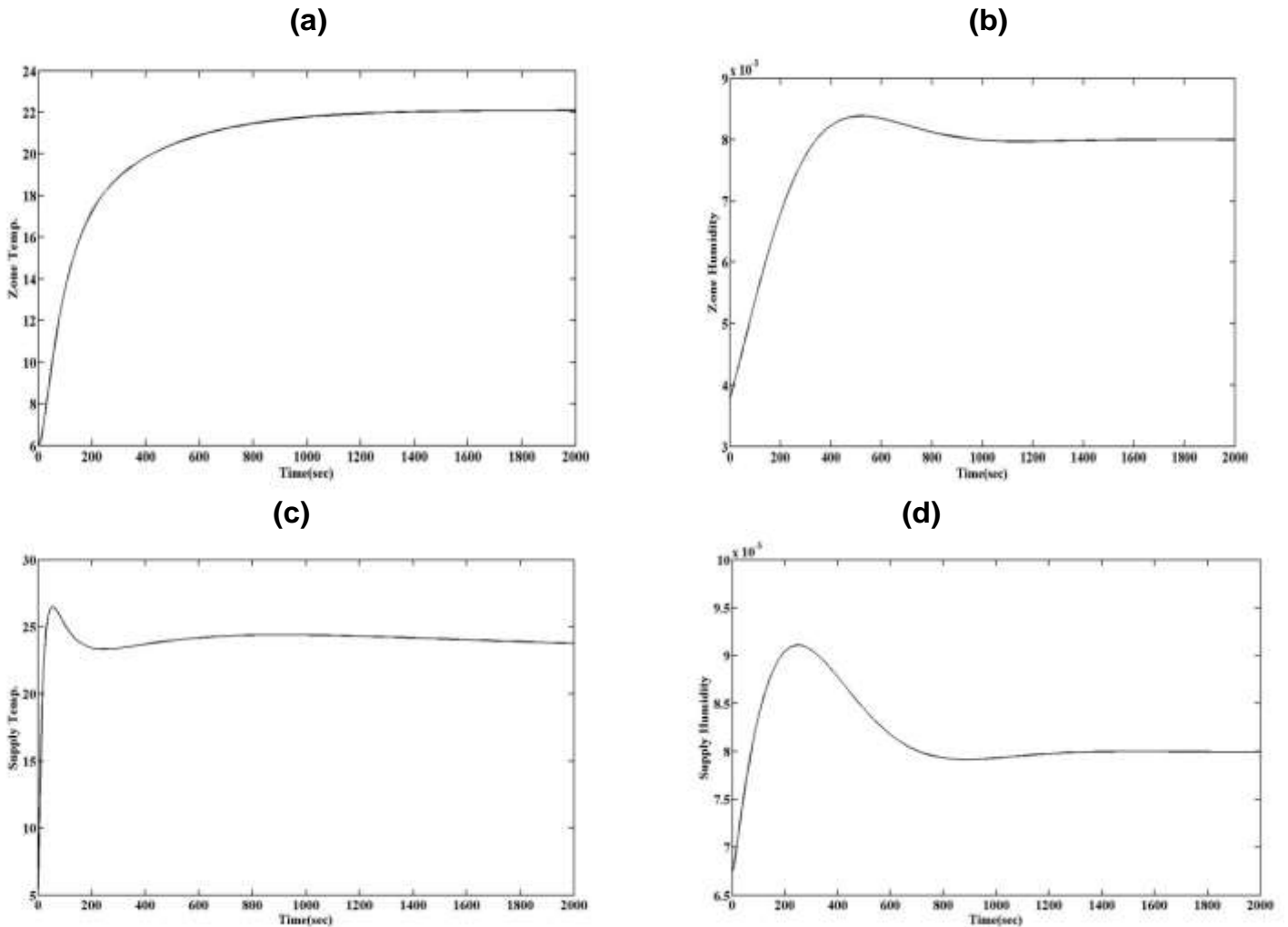


Figure 1. (a) Temperature of the controlled zone in winter operation season by PID controller. (b) Humidity ratio of the controlled zone in winter operation season by PID controller. (c) Supply air temperature of the controlled zone in winter operation season by PID controller. (d) Supply humidity ratio of the controlled zone in winter operation season by PID controller.

The nodes in a directed graph are representative of concepts and also the causal relationships between concepts are illustrated by graph's edges (Aguilar, 2005). The value of each concept shows the degree of activation of each concept at particular time (Aguilar, 2005). According to above mentioned the value of causal relationships between concepts should be taken values in interval $[-1, 1]$. The value of -1 indicates the strongly negative effect, $+1$ shows strongly positive effect and 0 has no effect. Referring to the values of edges, the causalities or relations are categorized into three types as if the relation of concepts takes positive value, express positive causality, if the relation of concepts takes negative value, express negative causality and if the relation of concepts takes zero value, express no relationship.

For one thing FCMs are hybrid model between fuzzy logic and neural networks (Aguilar, 2005). In other words,

FCMs are defined as a fuzzy-graph structure with existence of systematic causal propagation, in particular forward and backward chaining (Stylios and Groumpos, 2000). In comparison of fuzzy rule based method by FCMs many of knowledge-extraction problems which are related to fuzzy rule based method could be prevented (Aguilar, 2005). The other advantages of FCMs in comparison by expert system or neural networks are its simplicity to use for representing structured knowledge, and also computation of inference by numeric matrix operation (Papageorgiou and Groumpos, 2005).

MATERIALS AND METHODS

Mathematical model of fuzzy cognitive map

Besides the graphical structure, FCM follows its mathematical model which consists of a $1 \times n$ state vector A which contains the

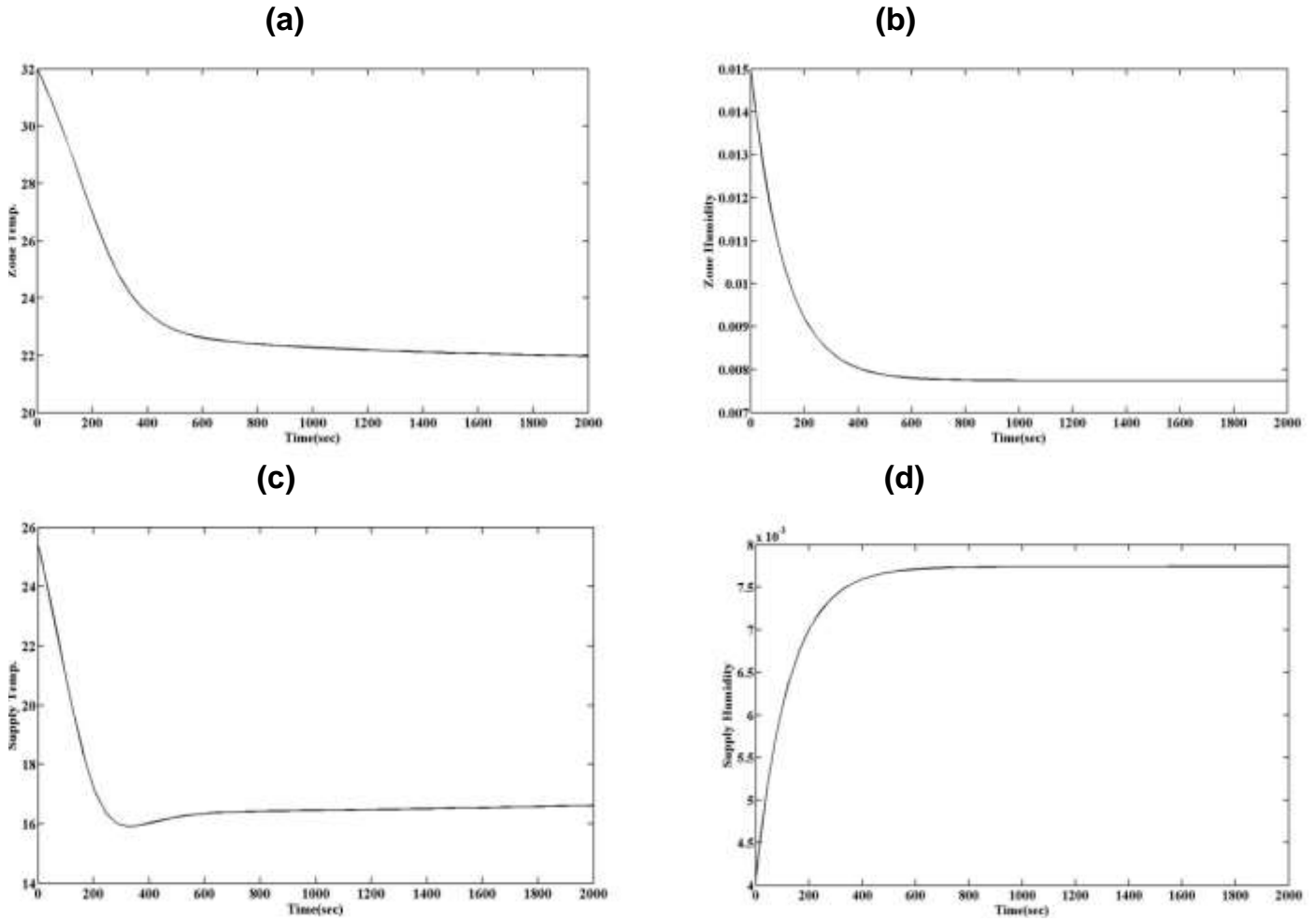


Figure 2. (a) Temperature of the controlled zone in summer operation season by PID controller. (b) Humidity ratio of the controlled zone in summer operation season by PID controller. (c) Supply air temperature of the controlled zone in summer operation season by PID controller. (d) Supply humidity ratio of the controlled zone in summer operation season by PID controller.

values of the n concepts and also an $n \times n$ weight matrix which includes the weights W_{ij} of the causality between concepts. The number of concepts is indicated by n . The value of each concept depends on linked concepts with proper weights and also the previous value of concept. After transferring the fuzzy values to the concepts, the $A_i^{new} = f(\sum A_j^{old} \times W_{ij}) + A_i^{old}$ (13) rule is used to calculate the activation level of A_i for each concept. A_i^{new} indicates the activation value of concept i at time $t+1$, A_i^{old} shows the activation value of concept j at time t and also f is a threshold function. There are two types of threshold functions which are applied in FCMs structure. The first one which is the unipolar sigmoid function to squash the content to the interval $[0, 1]$ is $f(x) = 1/(1+e^{-x})$ (14) and the second one which has been utilized to transform the content in the interval $[-1, 1]$ is $f(x) = \tanh(x)$ (15). The threshold function is chosen based on the used method to describe the concepts (Stylios and Groumos, 2004).

Applying the FCM controller on HVAC system

Based on construction of FCM, describing the concepts according to the goals, activities or state and characteristic of the system are needed. Referring to the HVAC system, inputs and outputs of the

system and the affecting parameters on inputs and outputs and also the system, two controllers are required one for heating model and the other for humidifier model in winter operation season and also two controllers for cooling coil and dehumidification coil in summer operation season. The concepts for heating model should be described as follow s:

- Concept 1: The temperature of the zone T_z , which is the output of the model.
- Concept 2: The T_w is temperature of the supplied water to the heating coil, which is the manipulated variable.
- Concept 3: The temperature out from the duct T_{out} , which is the output of the duct model.

The concepts for humidifier model should be described as follows:

- Concept 1: The humidity of the zone W_z , which is the output of the model.
- Concept 2: The W_{si} is humidity ratio of the supply air to the humidifier in, which is the manipulated variable.
- Concept 3: The humidity ratio out from the humidifier W_h , which is the output of the humidifier model.

The concepts for cooling model should be described as follows:

Concept 1: The temperature of the zone T_z , which is the output of the model.

Concept 2: The T_{w1} is temperature of water in cooling coil, which is the manipulated variable.

The concepts for dehumidifying model should be described as follows:

Concept 1: The humidity ratio of the zone W_z , which is the output of the model.

Concept 2: The T_{w2} is temperature of water in dehumidifying coil, which is the manipulated variable.

The impacts of the concepts are shown by weight matrix. The weight matrix is a $n \times n$ matrix which n is the number of concepts and impact of each concept on the others is a number in an interval $[-1, +1]$. The connection between concepts for heating model controller is as follows:

Linkage 1: It connects concept 1 (zone temperature T_z) with concept 2 (supply temperature of water T_{wi}). When the value of T_z increases, the value of T_{wi} increases and vice versa.

Linkage 2: It connects concept 1 (zone temperature T_z) with concept 3 (temperature out from the duct T_{out}). When the value of T_z increases, the value of T_{out} increases and vice versa.

Linkage 3: It connects concept 2 (supply temperature of water T_{wi}) with concept 1 (zone temperature T_z). When the value of T_{wi} increases, the value of T_z increases and vice versa.

Linkage 4: It connects concept 2 (supply temperature of water T_{wi}) with concept 2 (supply temperature of water T_{wi}). When the value of T_{wi} increases, the value of T_{wi} increases and vice versa.

Linkage 5: It connects concept 3 (temperature out from the duct T_{out}) with concept 1 (zone temperature T_z). When the value of T_{out} increases, the value of T_z increases and vice versa.

Linkage 6: It connects concept 3 (temperature out from the duct T_{out}) with concept 2 (supply temperature of water T_{wi}). When the value of T_{out} increases, the value of T_{wi} increases and vice versa.

The connection between concepts for humidifier model controller is as follows:

Linkage 1: It connects concept 1 (zone humidity W_z) with concept 2 (supply humidity ratio to humidifier W_{si}). When the value of W_z increases, the value of W_{si} increases and vice versa.

Linkage 2: It connects concept 1 (zone humidity W_z) with concept 3 (humidity ratio out from the humidifier W_h). When the value of W_z increases, the value of W_h increases and vice versa.

Linkage 3: It connects concept 2 (supply humidity ratio to humidifier W_{si}) with concept 1 (zone humidity W_z). When the value of W_{si} increases, the value of W_z increases and vice versa.

Linkage 4: It connects concept 2 (supply humidity ratio to humidifier W_{si}) with concept 2 (supply humidity ratio to humidifier W_{si}). When the value of W_{si} increases, the value of W_{si} decreases and vice versa.

Linkage 5: It connects concept 3 (humidity ratio out from the humidifier W_h) with concept 1 (zone humidity W_z). When the value of W_h increases, the value of W_z increases and vice versa.

Linkage 6: It connects concept 3 (humidity ratio out from the humidifier W_h) with concept 2 (supply humidity ratio to humidifier W_{si}). When the value of W_h increases, the value of W_{si} decreases and vice versa.

Linkage 7: It connects concept 3 (humidity ratio out from the humidifier W_h) with concept 3 (humidity ratio out from the humidifier W_h). When the value of W_h increases, the value of W_h decreases and vice versa.

The connection between concepts for cooling model controller is as

follows:

Linkage 1: It connects concept 1 (zone temperature T_z) with concept 1 (zone temperature T_z). When the value of T_z increases, the value of T_z increases and vice versa.

Linkage 2: It connects concept 1 (zone temperature T_z) with concept 2 (temperature of water in cooling coil T_{w1}). When the value of T_z increases, the value of T_{w1} increases and vice versa.

Linkage 3: It connects concept 2 (temperature of water in cooling coil T_{w1}) with concept 1 (zone temperature T_z). When the value of T_{w1} increases, the value of T_z decreases and vice versa.

Linkage 4: It connects concept 2 (temperature of water in cooling coil T_{w1}) with concept 2 (temperature of water in cooling coil T_{w1}). When the value of T_{w1} increases, the value of T_{w1} decreases and vice versa.

The connection between concepts for dehumidifier model controller is as follows:

Linkage 1: It connects concept 1 (zone humidity W_z) with concept 1 (zone humidity W_z). When the value of W_z increases, the value of W_z increases and vice versa.

Linkage 2: It connects concept 1 (zone humidity W_z) with concept 2 (water temperature of the dehumidifying coil T_{w2}). When the value of W_z increases, the value of T_{w2} increases and vice versa.

Linkage 3: It connects concept 2 (water temperature of the dehumidifying coil T_{w2}) with concept 1 (zone humidity W_z). When the value of T_{w2} increases, the value of W_z decreases and vice versa.

Linkage 4: It connects concept 2 (water temperature of the dehumidifying coil T_{w2}) with concept 2 (water temperature of the dehumidifying coil T_{w2}). When the value of T_{w2} increases, the value of T_{w2} decreases and vice versa.

According to the structure of FCMs, the values of the concepts correspond to the real measurements values that have been transformed in the interval $[0, 1]$. The measurement values are transferred by the transformation mechanism to their representative values of concepts. The chosen transformation mechanism (Kim et al., 2008) is:

$$g(s_i^t) = \begin{cases} 0, & \text{if } s_i^t < a_i \\ (s_i^t - a_i) / (2(m_i - a_i)), & \text{if } a_i \leq s_i^t \leq m_i \\ 0.5 + (s_i^t - m_i) / (2(b_i - m_i)), & \text{if } m_i < s_i^t \leq b_i \\ 1, & \text{if } s_i^t > b_i \end{cases}$$

Where:

s_i^t =observed value of the i th state at time t ; $a_i = \min_{t \in T} \{ s_i^t \}$; $b_i = \max_{t \in T} \{ s_i^t \}$; $m_i = \text{average}_{t \in T} \{ s_i^t \}$.

The initial vector of FCM is structured by transformation of initial measurement values of HVAC system. Then FCM starts to simulate the behavior of the process by equations (13) and (14). On the other words, the values of concepts are calculated at each running step of the FCM by considering that each running step at FCM is defined as time step. After few simulation steps, the values of concepts do not change. When the FCM reaches to this mentioned step, the final values of the concepts should be transformed to the real values and applied to the actuators. In spite of the advantageous of FCMs in designing to control the complicated and complex nonlinear systems, the most considerable weak point of FCMs are their potential to convergence to the undesired steady state is obvious (Papageorgiou and Groumpos, 2004). Learning ability of the FCMs is the best way to solve the mentioned problem.

By updating the strengths of causal links the values of concepts approach to the desired steady states (Lu et al., 2010).

Applying learning method on fuzzy cognitive map

Here, implementing the learning method is considered. Whereas the weakness of FCM are discussed in last section, adding learning method is an appropriate solution to convergence the results to the desired steady state. Among the different learning strategies which are used to train the weight matrix, the δ learning method is preferred. Referring to Lu et al. (2010), the δ learning method is a sort of supervised learning. According to Lu et al. (2010), reason for choosing this learning method are avoiding from low convergence speed, large iterative number and complexity of algorithm. On the other words, the other learning methods like genetic algorithm (GA), particle swarm optimization (PSO) or unsupervised learning's are disadvantageous due to the invariant weights, low learning speed, complexity of calculation and large number of iteration steps. Therefore, applying supervised learning on FCM due to the fast convergence make more suitable the control procedure to the online real-time controlling (Lu et al., 2010). Chosen learning method, the supervised δ learning rule (Lu et al., 2010) is $W_{ij}(K+1) = W_{ij}(K) + \Delta W_{ij}(K)$ which is $\Delta W_{ij}(K) = \eta A_i(K) A_j(K) (1 - A_j(K)) (d_j - A_j(K))$.

Where:

d_j = The expected value of input node j ; A_i = The state value of nodes connecting with this input node; A_j = The state value of input node j ; $\eta = \eta \in [0,1]$ is learning rate; K = The iteration step.

RESULTS AND DISCUSSION

In this research, the FCM method is utilized as a controller to control the parameters of zone temperature and zone humidity. The simulation results by MATLAB software show the comparison of the PID controller which is used in Tashtoush et al. (2005) with FCM controller for controlled variables of zone temperature and zone humidity respectively and for control variables supply air temperature and supply humidity ratio respectively. The comparison of the results of simulation by applying FCM controller and also PID controller in winter operation season got the below results. Figures 1 and 3 shows the responses of the HVAC system by implementing PID controllers and FCM controllers respectively in winter operation season.

Figure 3a shows the zone air temperature (T_z) which is controlled by discussed FCM controller in winter operation season. The air temperature increases slowly and exponentially in approximately 1000s to obtain to the 22°C which is set point value with small error. Figure 3(b) demonstrates the humidity ratio of the zone (W_z). It is clear that from the figure that the humidity ratio of the zone increases from 0.0039 to 0.0081 kg/kg and stabilizes in approximately 700 s with small error. Figure 3(c) shows the supplied air temperature (T_s) in winter operation season. The supplied air temperature increases softly from 5 to 24°C and stabilizes to 24°C in about 700 s. Figure 3(d) illustrates the supplied humidity ratio of the zone (W_s). It is clear that from the figure that

the humidity ratio of the zone rises rapidly from 0.0068 to 0.0081 kg/kg to reach and stabilizes to the steady state value of 0.008 kg/kg in about approximately 300 s with a very small error.

Figure 1(a) illustrates the zone air temperature (T_z) which is controlled by mentioned PID controller in winter operation season. The air temperature increases slowly and exponentially in approximately 1200 s to obtain to the 22°C which is set point value with small error. Figure 1(b) demonstrates the humidity ratio of the zone (W_z). It is clear that from the figure that the humidity ratio of the zone increases to 0.0085 kg/kg then decreases until stabilizes to obtain to the 0.008 kg/kg which is set point value in approximately 1000 s without almost any error. Figure 1(c) shows the supplied air temperature (T_s). The supplied air temperature increases to 27°C at the beginning and then decreases until stabilizes to 24°C. Figure 1(d) illustrates the supplied humidity ratio of the zone (W_s). It is clear that from the figure that the humidity ratio of the zone rises rapidly to 0.0093 kg/kg then declines smoothly to reach and stabilizes to the steady state value of 0.008 kg/kg in about approximately 1400 s.

In winter operation seasons results; the important improvement by FCM controllers is the cancellation of overshoots and undershoots which have seen on the Tashtoush et al. (2005) work. Referring to the achieved outcomes or outputs of the system, clearly the author designed control systems which is FCM one are smoother than the PID one. On the other words, in spite of the fact that the PID controllers are more advantageous and practical controllers, the outputs of the FCM controllers are smooth, but in Tashtoush et al. (2005) work, the outputs of some parts of the system have overshoot or undershoot before achieving to the desired set point value. It is clear that, by cancelling overshoot and undershoot, a part of energy which is consumed to produce them is saved and in addition using FCM controllers which are saved the energy by setting the suitable initial values for the system. The total consuming energy by PID controller is 15.295×10^4 in 2000s and 14.82×10^4 in same time for FCM one. The difference between two controllers shows 4.75% saving energy by FCM one. Comparison the results by PID and FCM controllers shows the FCM controllers are faster than PID one. The steady state is occurred sooner in FCM controller versus PID one. Comparison the results of the robustness of the PID and FCM controllers shows the FCM controllers are more robust than PID one. The steady state is occurred with negligible value in FCM controller versus PID one with small settling time in compare with PID one.

Moreover, the comparison of the results of applying FCM controller and PID one for summer operation season got the below results. Figures 2 and 4 shows the responses of the HVAC system by implementing PID controllers and FCM controllers respectively in summer operation season.

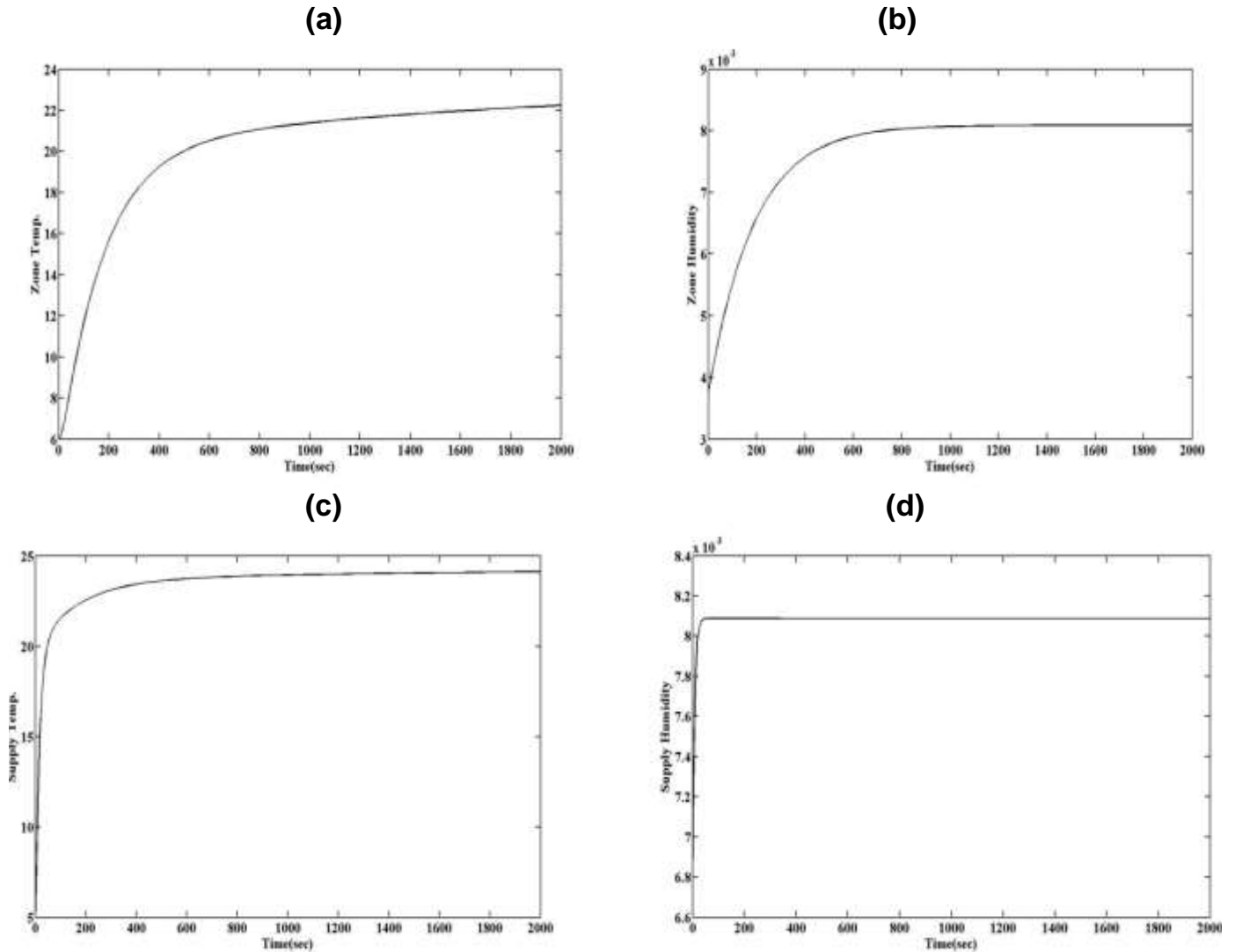
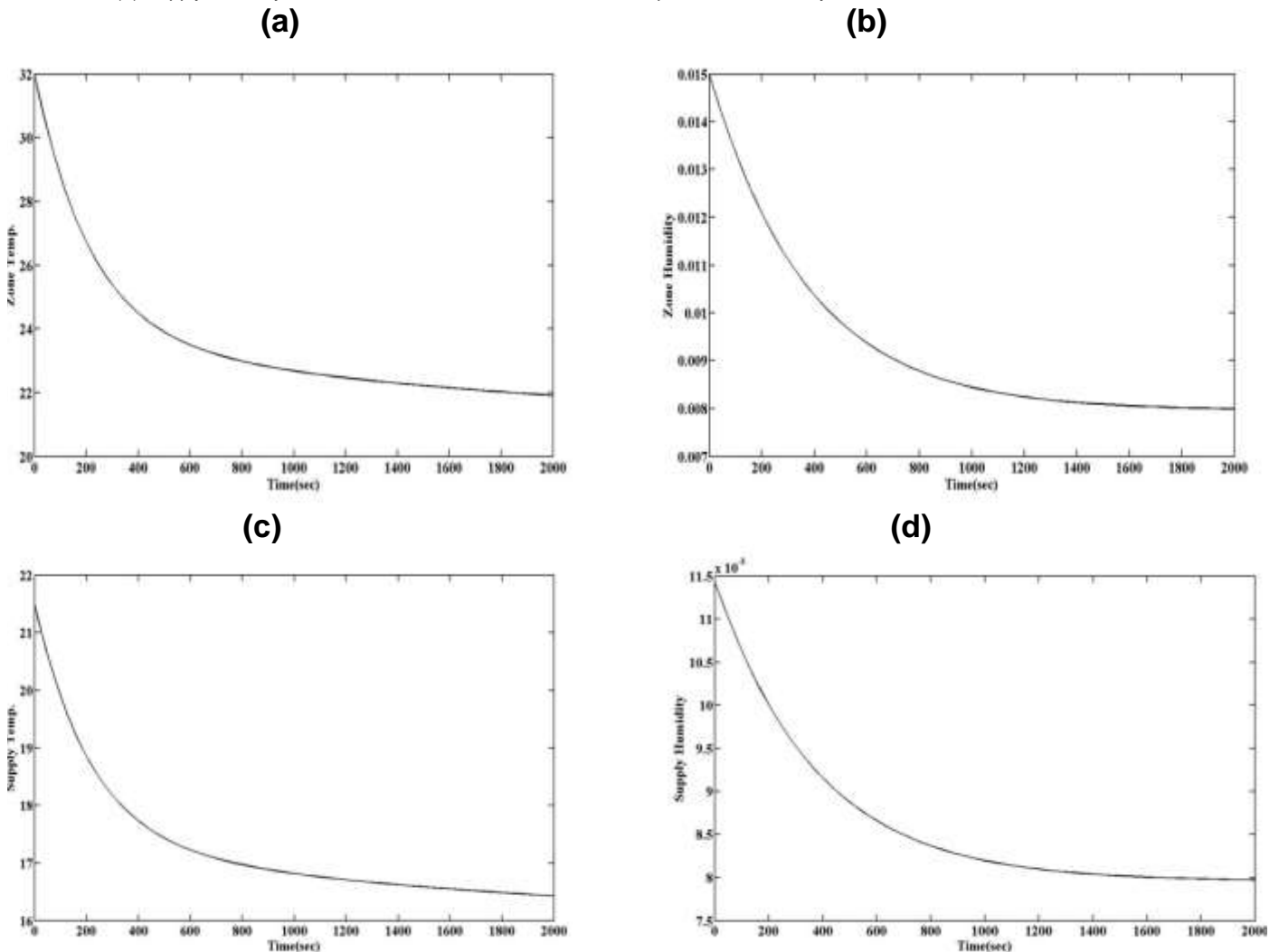


Figure 3. (a) Temperature of the controlled zone in winter operation season by FCM controller. (b) Humidity ratio of the controlled zone in winter operation season by FCM controller. (c) Supply air temperature of the controlled zone in winter operation season by FCM controller. (d) Supply humidity ratio of the controlled zone in winter operation season by FCM controller.

Figure 4a shows the zone air temperature (T_z) which is controlled by mentioned FCM controller in summer operation season. The air temperature declines smoothly and exponentially to obtain to the 22°C which is set point value in about 1200 s with a small error. Figure 4b illustrates the humidity ratio of the zone (W_z). The humidity ratio of the zone decreases smoothly to obtain to the 0.008 kg/kg which is set point value in approximately 1000 s with negligible error. Figure 4c demonstrates the supplied air temperature (T_s) in summer operation season. The supplied air temperature decreases smoothly and stabilizes to 16.4°C. Figure 4(d) shows the supplied humidity ratio of the zone (W_s). It is obvious that from the figure that the humidity ratio of the zone declines slowly from 0.0115 to 0.008 kg/kg and stabilizes in about approximately 950 s.

Figure 2a shows the zone air temperature (T_z) which is controlled by mentioned PID controller in summer operation season. The air temperature decreases slowly and exponentially to obtain to the 22°C which is set point value in approximately 1700 s with a small error. Figure 2(b) illustrates the humidity ratio of the zone (W_z). It is obvious that from the figure that the humidity ratio of the zone declines smoothly to obtain to the 0.008 kg/kg which is set point value in approximately 1000 s with a small error. Figure 2c demonstrates the supplied air temperature (T_s). The supplied air temperature decreases from 25.5 to 16°C at the beginning until 350 s and then increases to 17°C. Figure 2d illustrates the supplied humidity ratio of the zone (W_s). It is obvious that from the figure that the humidity ratio of the zone rises smoothly from 0.0044 to 0.0078 Kg/Kg and stabilizes to

Figure 4. (a) Temperature of the controlled zone in summer operation season by FCM controller. (b) Humidity ratio of the controlled zone in summer operation season by FCM controller. (c) Supply air temperature of the controlled zone in summer operation season by FCM controller. (d) Supply humidity ratio of the controlled zone in summer operation season by FCM controller.



0.0078 kg/kg in about approximately 1200 s.

In summer operation season; the remarkable point is the cancellation of overshoots and undershoots which have seen on the Tashtoush et al. (2005) work. Based on the obtained results or outputs of the system, obviously the FCM designed control systems are smoother than the PID one. On the other words, despite the fact that the PID controllers are more useable controllers, the outputs of the FCM controllers are smooth, but in the Tashtoush et al. (2005) work, the outputs of some parts of the system have overshoot or undershoot before reaching to the desired value. It is obvious that, by cancelling overshoot and undershoot; a part of energy which is used to produce them is saved and also using FCM controllers which is saved the energy by decreasing the initial values. The total consuming energy by PID controller is 8.618×10^4 in 2000 s and 6.4×10^4 in same time for

FCM one. The difference between two controllers shows 22.18% saving energy by FCM one. Comparison the results of the robustness for the PID and FCM controllers depicts the FCM controllers are more robust than PID one. The steady state is happened with negligible value in FCM controller versus PID one with small settling time in compare with PID one.

The comparison of the results of simulation by applying FCM controller, it is obvious that, in contrast with PID controller (Tashtoush et al., 2005), the FCM one has no overshoot or undershoot. Obtaining to cancel the overshoot and undershoot decrease the pressure to the system and also decline the energy consumption.

The results of the simulation shows that, this method has the features like simple algorithm, small number of iteration steps and good robustness and it will be suitable for real time control of complex industrial process.

The learning method is implemented to update the weight matrix to get better results and decrease the cycles. Through using a δ learning rule, FCM has a reason process which is similar to human does, and then an online real-time control is achieved.

Conclusions


In this work, the comparisons of the Fuzzy Cognitive Maps method to control versus PID controller have been done. As mentioned previously, decreasing the consuming energy by HVAC system due to the eliminating of overshoot and undershoot on the supply temperature and supply humidity is obtained and also decreasing on the supply temperature in fewer runtime is achieved. Good robustness is another advantage of using this method and also the simple mathematic model of the controller which does not involve with the mathematical model of the system according to the characteristics of FCMs. It is clear that, this method is more efficient in saving energy and optimizing the balance between thermal comfort and energy usage to improve thermal comfort issue and Energy efficiency. The simulation results shows, for designing a nonlinear robust Closed-loop real-time on-line learning ability controller with simple control algorithm, the FCMs could be a better choice among the others.

Conflict of Interests

The authors have not declared any conflict of interests.

REFERENCES

- Aguilar J (2005). A survey about fuzzy cognitive maps papers (Invited paper). *Int. J. Comput. Cog.* 3(2): 27-33.
- Aguilar J (2003). A dynamic fuzzy-cognitive-map approach based random neural networks. *Int. J. Comput. Cog.* 1(4):91-107.
- Bertolini M (2007). Assessment of human reliability factors: A fuzzy cognitive maps approach. *Int. J. Ind. Ergonom.* 37:405-413.
- Clark DR, Hurley CW, Hill CR (1985). Dynamics models for HVAC system components. *ASHRAE T* 91(1):737-751.
- Elmahdy AH, Mitalas GP (1977). Simple model for cooling and dehumidifying coils for use in calculating energy requirements for buildings. *ASHRAE T* 83(2):103-117.
- Ghazanfari M, Alizadeh S, Fathian M, Koulouriots DE (2007). Comparing simulation annealing and genetic algorithm in learning FCM. *J. Appl. Math. Comp.* 192:56-68.
- Huang W, Zaheeruddin M, Cho S (2006). Dynamic simulation of energy management control functions for HVAC systems in buildings. *Energy Convers. Manage.* 47:926-943.
- Kasahara M, Kuzuu Y, Matsuba T, Hashimoto Y, Kamimura K, Kurosu S (2000). Stability analysis and tuning of PID controller in VAV systems. *ASHRAE T* 106(2):285-296.
- Khor S, Khan MS (2003). Scenario Planning using Fuzzy Cognitive Maps. *Proc. ANZIS2003 8th Australian and New Zealand Intelligent Information Systems Conference*, pp. 311-316.
- Kim M, Kim C, Hong S, Kwon I (2008). Forward-backward analysis of RFID-enabled supply chain using fuzzy cognitive map and genetic algorithm. *Expert Syst. Appl.* 35:1166-1176.
- Lei J, Hongli L, Cai W (2006). Model Predictive Control Based on Fuzzy Linearization Technique For HVAC Systems Temperature Control. *IEEE*, pp. 1-5.
- Lu W, Yang J, Li Y (2010). Control method based on Fuzzy cognitive map and its applications district heating network. *International Conference on Intelligent Control and Information Processing (ICICIP 2016) August 13-15, Dalian, China.*
- Papageorgiou E, Groumpos P (2005). A new hybrid method using evolutionary algorithms to train Fuzzy Cognitive Maps. *Appl. Soft. Comput.* 5(4):409-431.
- Papageorgiou E, Groumpos P (2004). Two-Stage Learning Algorithm for Fuzzy Cognitive Maps. *IEEE Int. Conf. Intell. Syst.* pp. 22-24.
- Stein B, Reynolds J, McGuinness W (2000). *Mechanical and electrical equipment for buildings.* Wiley.
- Stylios D, Groumpos P (2004). Modeling complex system using Fuzzy Cognitive Maps. *IEEE Syst. Man. Cyb.* 34(1).
- Stylios C, Groumpos P (2000). Fuzzy cognitive maps in modeling supervisory control systems. *J. Intell. Fuzzy Syst.* 8:83-98.
- Tachwali Y, Refai H, Fagan J (2007). Minimizing HVAC Energy Consumption Using a Wireless Sensor Network. *Industrial Electronics Society, 2007, IECON 2007, 33rd Annual Conference of the IEEE*, p. 439.
- Tashtoush B, Molhim M, Al-Rousan M (2005). Dynamic model of an HVAC system for control analysis. *Energy* 30:1729-1745.
- Wang J, An D, Lou C (2006). Application of fuzzy-PID controller in heating ventilating and air-conditioning system. *IEEE*, pp. 2217-2222.



International Journal of Physical Sciences

Related Journals Published by Academic Journals

- *African Journal of Pure and Applied Chemistry*
- *Journal of Internet and Information Systems*
- *Journal of Geology and Mining Research*
- *Journal of Oceanography and Marine Science*
- *Journal of Environmental Chemistry and Ecotoxicology*
- *Journal of Petroleum Technology and Alternative Fuels*



academicJournals